U.S. DEPARTMENT OF COMMERCE
National Oceanic and Atmospheric Administration
Environmental Research Laboratories

NOAA Technical Memorandum ERL NSSL-56

PILOT CHAFF PROJECT AT NSSL

Edward A. Jessup

National Severe Storms Laboratory
Norman, Oklahoma
November 1971

TABLE OF CONTENTS

LIST OF FIGURES

A PILOT CHAFF PROJECT AT NSSL

Edward A. Jessup
National Severe Storms Laboratory
Norman, Oklahoma

Chaff was released near thunderstorms on four occasions during 1969. These experiments tested the feasibility of obtaining and analyzing chaff data near thunderstorms at mid- and low-levels of the atmosphere. A discussion of chaff trajectories and speculation on air flow near these thunderstorms is presented.

1. INTRODUCTION

During recent years, interest has grown concerning the relationship between severe thunderstorms and environmental air flow. Before World War II, most meteorologists agreed with Humphreys (1940) that the velocity of a thunderstorm is nearly the velocity of the atmosphere in which the bulk of the cloud is located. Since then, thunderstorm studies have become more sophisticated with the advent of radar, high altitude aircraft, and rawinsonde equipment. As Fankhauser (1964) mentions, accumulated evidence shows that small uniform, nonpropagating storms frequently move with the winds at a particular level (usually near 700 mb), but propagating cumulonimbi of various sizes do not. Thunderstorms have been observed to merge (Stout and Hiser, 1955), split (Fujita and Grandoso, 1968), and move to the right and left of the mean flow (Newton and Katz, 1958; Harrold, 1966; and Hammond, 1967). This suggests that the interaction of thunderstorm circulation with environmental flow is reflected in storm motion.

Three possible views of the general relationship between strong thunderstorms and environmental flow are (1) the thunderstorm acts as a barrier to environmental flow; (2) air flows through the thunderstorm with little resistance; or (3) thunderstorms neither are rigid barriers to environmental flow, nor does air flow through them freely.

One of the tasks of the Storm Morphology and Dynamics Project at the National Severe Storms Laboratory (NSSL), Norman, Oklahoma, has been collecting data to examine these viewpoints. One technique involves the tracking of chaff bundles released in the vicinity of large thunderstorms. Fankhauser (1968) discussed a chaff experiment performed near NSSL in which 13 bundles were released at 500 mb, both upwind and downwind of a mature right-moving severe thunderstorm. His analysis indicated that most of the bundles tended to flow around the storm. A single bundle was observed, however, to merge with the precipitation echo. These observations suggested to him that the mature thunderstorm acted as an effective barrier to middle tropospheric flow, although some of the ambient air simultaneously entered the thunderstorm.

In the spring of 1969, Weather Science, Inc., under contract with ESSA (now NOAA), released chaff from aircraft near thunderstorms when requested by NSSL. Each chaff package contained approximately 400,000 aluminum-coated glass fibers. Each fiber was approximately 1 mil in diameter and 10.7 cm long, the wavelength of the WSR-57 radar at NSSL. Manufacturer[1] specifications indicate a radar cross section of 5000 ft^2 per package. Tests performed by the U.S. Air Force and independently by NSSL, indicated that individual dry fibers have a terminal velocity near 0.50 kt when in still air. Additional tests at NSSL indicated that wet fibers have a terminal velocity near 0.80 kt. No data are available concerning fall rates when icing takes place. All chaff experiments were designed to minimize icing influences.

Chaff positions were recorded by time-lapse photography of a WSR-57 PPI scope. The time interval between each filmed scan was near 45 sec. The NSSL radar display shows echo intensities contured at reflectivity factor (Z_e) intervals of a factor of 10, from 10 to $10^6 mm^6 m^{-3}$. (All Z_e factor units in this paper are $mm^6 m^{-3}$ and later references will not include them.) The NSSL radar system has been described by Wilk et al. (1968) and by Sirmans et al. (1970).

Chaff was released near thunderstorms four times during May and June, 1969; May 25, May 29, June 23, and June 25. The discussion of these experiments is in order of significance and happens to be in reverse chronological order.

---

[1]Lundy Electronics and Systems, Inc., Glen Head, New York 11545.

2. SYNOPTIC CONDITIONS ON 25 JUNE 1969

The atmosphere over Oklahoma early on 25 June 1969 was moderately conducive to severe thunderstorm formation. Surface and 500-mb synoptic charts of an intense low over the Great Plains are shown in figure 1. Flow toward the low was bringing warm moist Gulf air across Oklahoma at low levels and dry air aloft, thus providing two important ingredients for severe thunderstorm development. The weak cold front entering northwestern Oklahoma during the morning (fig. 1a) acted as a lifting mechanism over central Oklahoma later during the day. This, with a minor trough aloft and surface heating, caused thunderstorms to form during the afternoon.

At 1455 (all times are CST) a thunderstorm formed about 60 n mi southwest of Oklahoma City and became severe as it moved to the northeast. Within an hour after it formed (1545), the storm began to move to the right of winds at most levels, as implied by the 1200 Tinker AFB hodogram (insert in fig. 2), and radar indicated that precipitation particles extended to 55,000 ft MSL. According to the *Storm Data* series published by the Department of Commerce, the storm was accompanied by several funnels and a small tornado that touched down near Choctaw, a suburb of Oklahoma City, and caused minor damage. Hail up to 2 inches in diameter and winds faster than 55 kt also occurred in nearby areas.

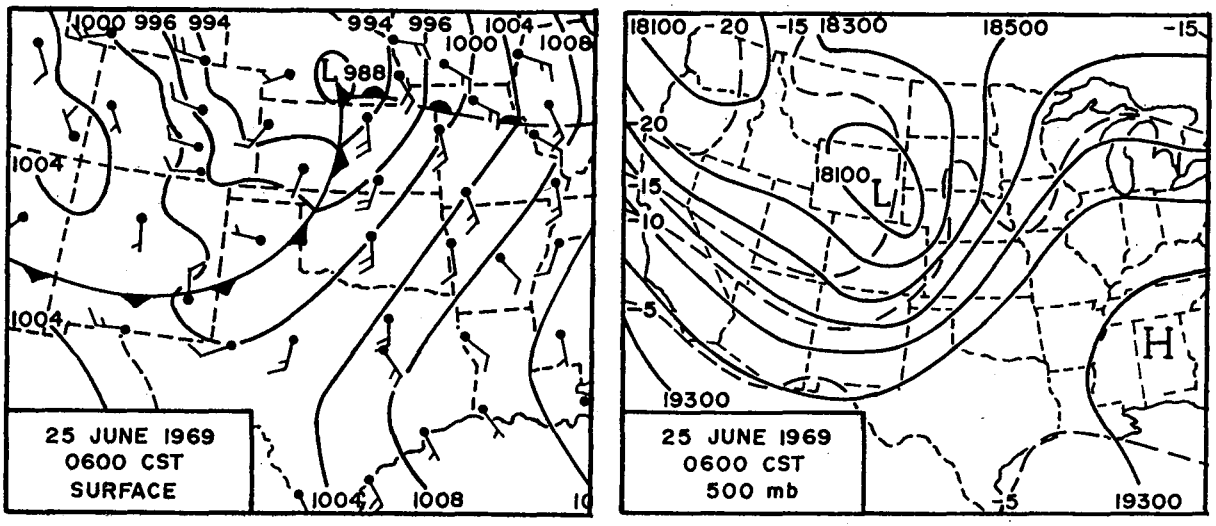

Figure 1. Synoptic charts before thunderstorm development.

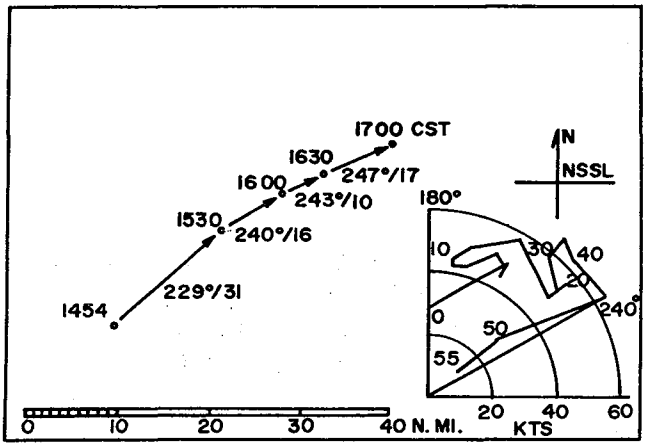

Figure 2. Trajectory of thunderstorm precipitation echo, 25 June 1969. The Tinker AFB hodogram 1200 is inserted at the right of the figure.

The thunderstorm had several structural features similar to those of the quasi-steady state SR (severe right) model of Browning (1964). The two most prominent were a hook-shaped echo (fig. 3a) and an extensive overhang in advance of the precipitation column appearing at 1637.

3. CHAFF TRAJECTORIES

3.1 Chaff Deployment

A single-engine Cessna with a cruising speed of 150 kt was used to place 11 bundles of chaff 5 to 10 n mi upwind from the thunderstorm. They were released between 1519 and 1553 at 15,000 ft MSL (average terrain near 1200 ft MSL), at 5 n mi intervals, except the first two bundles which were separated by 3 n mi. Nine were released in an "L"-shaped pattern along the northwestern and southwestern sides of the thunderstorm, as indicated in figures 4 a,b, and c. Two bundles, 10 and 11, were dropped west of bundle 9 but do not appear in figure 4.

The WSR-57 radar antenna tilt was fixed at 2° until all chaff was ejected. As bundle 11 was dropped, an automatic antenna tilt sequence from 1° to 4° at 1° increments was initiated. At first, each chaff bundle appeared as a point on radar. After 30 min, however, several bundles had intensity contours of $Z_{e\ max} = 10^3$, as shown in figure 4.

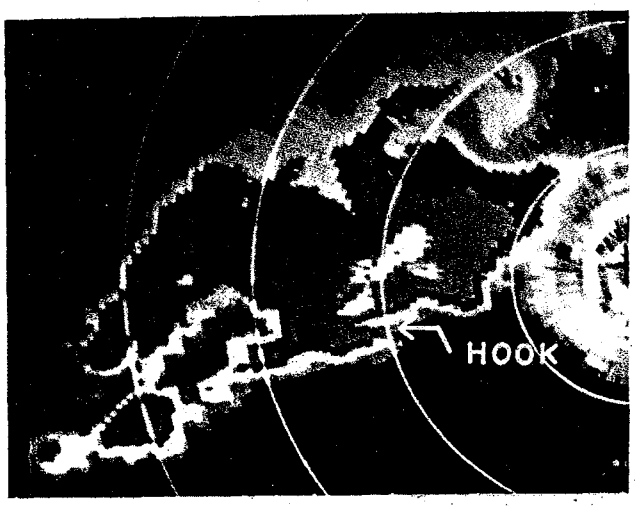

Figure 3a. Integrated contoured NSSL WSR-57 radar display for 25 June 1969, 1637 CST. Antenna elevation is 3° with range marks at 10 n mi intervals.

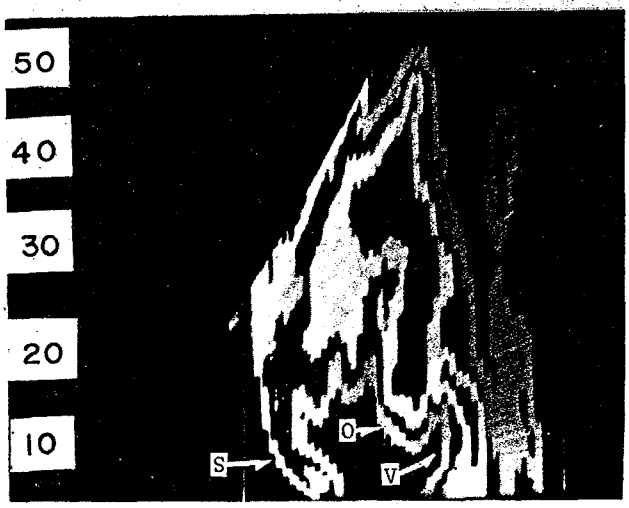

Figure 3b. Integrated and contoured MPS-4 range-height radar display at 1637 CST. The vault is shown by V, the overhang by O, and a precipitation streamer descending from the anvil to the surface is marked by S (from Lemon, 1970).

3.2 Chaff Echoes

Chaff was expected either to flow around the thunderstorm or to move into it and not be seen again. Surprisingly, however, of nine chaff bundles whose echoes merged with the precipitation echo, three were apparently associated with chaff-like echoes that later emerged from the downwind side of the storm. The following discussion explains why these echoes are considered to be chaff. It will be shown that echoes known to be chaff and the emerging chaff-like echoes behaved similarly and not as precipitation echoes typically behave.

The horizontal motion of the chaff and the chaff-like echoes is revealed by the WSR-57 time-lapse film. Chaff bundles 1 and 2 did not enter the precipitation echo, thus allowing chaff-like echoes to be compared with echoes known to be chaff. Two chaff-like echoes traveled within the

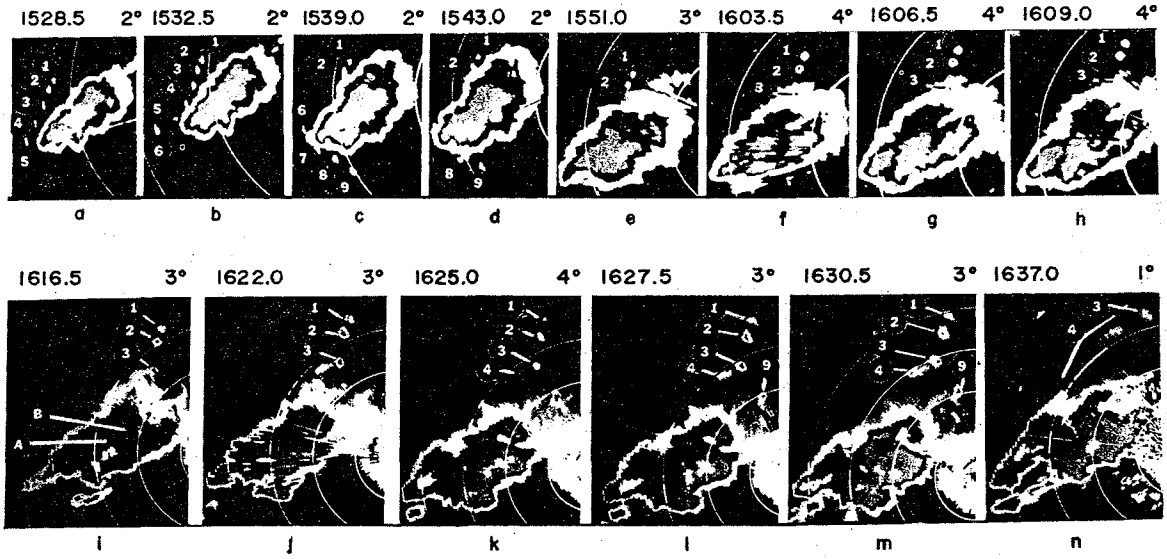

Figure 4. WSR-57 PPI displays of chaff and precipitation at NSSL 25 June 1969. Time are indicated to the nearest half-minute at the top of each photo. Radar antenna elevation in degrees is at the top right. Chaff is numbered adjacent to the chaff echo. The lettered arrows (after Lemon, 1970) indicate the following: A=the low reflecting intrusion of the eddy vortex; B=the high reflectivity crescent of the vortex.

precipitation echo, emerged from it, and then moved away at a velocity similar to chaff. It seems possible to track chaff in precipitation since chaff tends to enhance the precipitation reflectivity enough to produce a region of greater reflectivity that could be followed from frame to frame.

Figure 4 helps to illustrate the movement and appearance of chaff and chaff-like echoes. Bundles 1 and 2 in figures 4a through 4m were followed continuously and can be seen to remain outside the precipitation echo. Both chaff (labeled 2) and chaff-like echoes (labeled 3 and 9) in figures 4b through 4m returned a maximum reflectivity value of $Z_e \approx 10^3$, as indicated by a small circular area. The chaff-like echoes were visible within the precipitation and were followed along a smooth and continuous path. The echo labeled 3 appears below bundle 2 at an indicated separation of 7 n mi in figure 4f, only 2 n mi greater than the initial separation of bundles 2 and 3. Figures 4f through 4m show that these bundles had a similar appearance on radar, moved similarly, and retained their relative separation as bundle 3 emerged from precipitation. Number 9 behaved likewise, as indicated by figures 4k through 4m.

One other chaff-like echo (labeled 4) initially appeared on radar at the downwind edge of the precipitation echo. Although figure 4n shows that it was plume-shaped and thus different from other chaff echoes, it traveled similar to numbers 1, 2, 3, and 9.

All echoes in question slowly decreased in intensity and altitude, but remained intact during the hour after chaff-like echoes emerged from the storm. Figure 5 is a graph of the radar heights at which chaff and chaff-like echoes returned maximum reflectivity. Curves labeled 1 and 2 pertain to echoes known to be chaff. Those numbered 3, 4, and 9 represent the chaff-like echoes.

Both chaff and chaff-like echoes had similar fall speeds that were significantly less than the terminal speed of precipitation with similar reflectivities in still air. This was discovered in the following way. Fall rates of chaff and chaff-like echoes are shown in figure 5. An estimate of the rainfall rate of similar reflectivities (average maximum reflectivity between 10^2 and 10^3) was determined from the relationship

$$Z_e = 200r^{1.6}$$

to be about 0.06 in hr^{-1}. The median raindrop diameter corresponding to this rainfall rate was determined to be 0.06 in from the drop-size spectra data collected by Mueller and Sims (1966). They obtained this spectra using photographs collected from a camera sampling raindrops of several sites across the world and under various rainfall regimes. The values cited here are the results obtained at Miami, Florida, during thunderstorm situations. A 0.06-in diameter

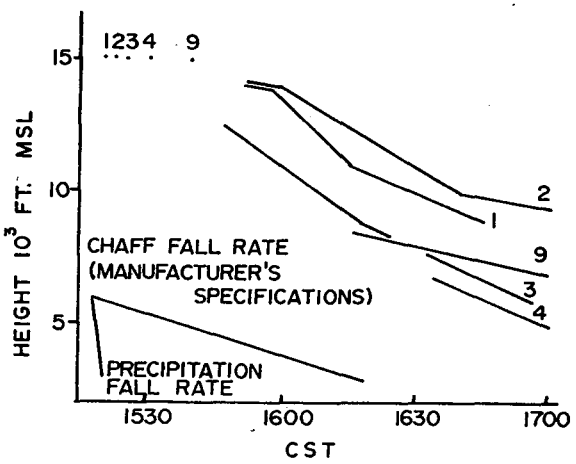

Figure 5. Chaff and precipitation fall rates. Numbered lines are chaff bundles 1, 2, 3, 4, and 9. The fall rate of precipitation with reflectivity similar to that of chaff is presented at the lower left.

droplet has a terminal velocity of near 10.8 kt, according to Gunn and Kinzer (1948). A comparison between the observed fall rates of the chaff and the chaff-like echoes (0.36 to 1.88 kt) and those estimated for precipitation (10.8 kt) indicated that precipitation fall rates were an order of magnitude greater.

Of course, both estimates are relative to still air. But, had the chaff-like echoes been precipitation, a large area of uniform upward air motion is then implied on the downwind side of the storm. Such a feature would have caused these echoes to intensify and increase in vertical extent. These echoes, however, behaved in the opposite sense. In light of the evidence discussed above, it is believed that the chaff-like echoes were indeed chaff.

3.3 Horizontal Chaff Trajectories

Chaff trajectories relative to the storm are superimposed on the approximate envelope of the precipitation echoes during the period from 1519 to 1645 in figure 6. The hatched shading is the envelope of precipitation echoes with reflectivities $Z_e \geq 10^4$. As noted before, bundles 1 and 2 were tracked continuously and remained outside the precipitation echo thus eliminating any doubt concerning their trajectories. Of the remaining nine bundles that disappeared into the storm, three were later tracked again (numbers 3,4, and 9). Time-lapse film, velocity computation, and extrapolation of chaff trajectories suggest that the three chaff fundles that emerged from the storm correspond the the like numbered bundles on the upwind side of the storm echo, as shown in figure 6.

Filmed PPI displays suggest that the chaff plume, number 4, was possibly composed of two bundles, perhaps 4 and 5, or 4 and 6. A reflectivity-volume product was formed for the plume and echo 2 by multiplying the average reflectivity of each echo times the volume it occupied. The reflectivity of number 2 was considered as representative of what was expected from just one bundle, since it remained outside the storm and intact. The volume was defined as the sum of the products of echo areal display at various antenna tilt angles times the average vertical depth equivalent to 1° of arc, the incremental angle between successive PPI photographs. The ratio of the reflectivity-volume products between the plume and 2 was about two, implying that the plume contained two bundles. Further discussion as to which two is presented later. Numbers 3 and 9 were similarly compared to number 2, and it appears that they were composed of only their original chaff.

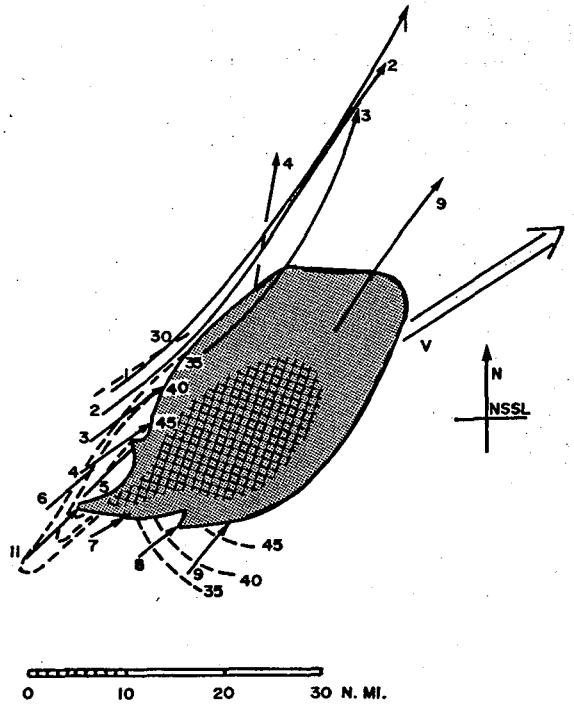

Figure 6. Chaff trajectories (solid) and isotachs (dashed) relative to composite precipitation echo. Thunderstorm motion is indicated by the double arrow.

Some of the considerations behind the echo labeling in figure 6 follow. Number 3 is discussed first. When the trajectory of the chaff echo appearing within the northwest side of the storm (fig. 4b) was extended backward to the southwest edge of the precipitation echo, it was found to be near the location where number 3 entered the storm. Both when within and emerging from precipitation, it had a velocity similar to that of number 3 before it entered the precipitation. It was labeled 3 for these reasons.

As number 3 left the storm, it was joined to the plume that trailed downward and back 20 n mi toward the storm (figs. 4*l*, m, and n). It seems likely that the plume was composed of numbers 4 and 5. They were nearest number 3 in space and time (number 6 was released later and upstream from 4 and 5) as they entered precipitation; and data in figure 6 suggests that 4 and 5 may have merged, since 5 was moving toward and slightly faster than 4. Although it is probable that the plume was composed of these two chaff bundles, it was designated as number 4 for convenience.

At about 1617, another chaff bundle reappeared within the precipitation echo and about 15 n mi east of the location of number 3 (fig. 4i). Evidence from filmed PPI displays suggests that this was bundle 9, which was released at the southern edge of the storm. Its velocity upon emerging

was similar to that of number 9 before it entered the thunderstorm, and a backward extension of its trajectory intersected with the edge of the precipitation echo near the location where 9 entered the storm. Numbers 6, 7, and 8 could have traveled the necessary distance at a reasonable speed to be the chaff in question, but it seems unlikely for the following reasons. The relative trajectory of number 6 was similar to that of numbers 4 and 5 when outside the precipitation echo; thus, it is reasonable to assume that it, too, experienced downward motion and dispersal similar to the plume. Number 7 entered the storm near the core of the echo where up-and downdrafts are expected. Had number 7 reappeared, numbers 8 and 9 would likely have been tracked again also. Similarly, if number 8 had reappeared, number 9 would have been expected to reappear. Only one bundle was in evidence, however. Numbers 10 and 11 were unlikely candidates because the speeds required for them to travel to where the chaff reappeared were significantly faster than those observed elsewhere, 75 and 180 kt, respectively. Thus, considering evidence cited above, the bundle emerging from the forward (northeast) flank of the storm was designated as number 9. One additional note: although figure 6 implies that bundle 9 traveled within precipitation with $Z_e \geq 10^4$, this probably did not happen since these reflectivities apparently occurred along the trajectory after the chaff moved past that region.

The remaining chaff, bundles 6, 7, 8, 10, and 11, apparently entered the storm and were not seen again. They entered where strong up and downdrafts probably were occurring near each other. It is reasonable to assume that these bundles either traveled upward and left the storm aloft or were forced down by heavy precipitation and/or downdrafts.

4. RELATIVE AIRFLOW

4.1 Airflow in General

Wind speeds relative to the precipitation echo appearing in figure 6 were derived from 5-min changes in chaff positions from 1525 to 1555. Isotachs were analyzed along the upwind side of the storm where chaff was dropped at 15,000 ft MSL. An isotach analysis downstream from the thunderstorm reveals that similar speeds were present there, but the analysis is not found in figure 6 because chaff at that side of the storm was present at various levels.

Discussion in this section indicates that this storm was well ventilated at midlevels except in a relatively small region near the hook echo where blocking was apparent. In the lee of the blocking vortex, there is some evidence of eddy generation.

Resistance to flow and thunderstorm ventilation are both indicated by the flow pattern appearing in figure 6. Nearly parallel flow was present entering and emerging from the right and left flanks of the storm where low reflectivity precipitation echoes were located. This observation, along with the high speed of the relative wind in the same regions, suggests that these portions of the storm were well ventilated. Resistance to air flow was found along the upwind side of the thunderstorm near the hook-shaped echo. The pattern resembles that found within fluid flow along the upflow side of a solid circular cylinder: diffluence was indicated by the separation of bundles 5 and 6 from bundles 7 and 8 on either side of the hook where a speed minimum appears in figure 6. The flow pattern is also consistent with the general observation that ambient flow is deflected around vortices; intense hook-shaped echoes have been related to cyclonic rotation (Fujita, 1958) and to vertical motion (Browning and Donaldson, 1963), which, in turn, has been related to blocking of environmental air flow (Hitchfield, 1960).

Similar flow patterns near thunderstorms have been suggested by others. Thunderstorm ventilation and resistance to flow was noted by Donaldson et al. (1969) and by Kraus (1970) in their investigation of the flow within an isolated right-moving severe thunderstorm near Marblehead, Mass. Wind components along the Doppler radar radial within that storm indicated that it was ventilated along both its up and downwind sides. Blocking by the updraft portion of the storm was inferred from regions of speed minima believed to be associated with wake phenomena.

The flow along some fringes of the June 25th storm was apparently smooth both inside and outside the precipitation echo. Remarks made by the aircraft pilot after chaff was ejected indicated that no turbulence was experienced, and radar indicated that chaff bundles 1, 2, 3, and 9 dispersed only slowly with time. This was true although vertical velocity estimates indicated that air near bundles 3 and 9 traveled downward after entering precipitation.

A more turbulent record, however, was indicated by the shape of number 4, which apparently traveled near echo reflectivities of $Z_e \approx 10^4$. After this bundle emerged from precipitation, it was plume-shaped and trailed downward

toward the storm from near 10,000 ft MSL (the same altitude as number 3) to about 5000 ft MSL for a distance of 20 n mi. Apparently this chaff was subjected to downward motion, vertical shear, turbulence, precipitation scavenging, or some combination of these.

Lemon (1970) studied another aspect of this storm during a period that overlaps this study. He observed that a convergent anticyclonic eddy vortex (fig. 7b) apparently developed and then emerged from the downwind side of the storm in the region between bundle number 9 and numbers 3 and 4. Number 9 had a tail (figs. 4ℓ and 4m) that was oriented nearly perpendicular to its direction of motion. It seems plausible that the tail was drawn away from the main body of chaff by the anticyclonic vortex (visible in figs. 4i through 4m) as its circulation increased to include air near bundle 9. Although the air near bundle 3 apparently moved downward after entering precipitation, it did not appear to be involved with the anticylonic circulation. Instead it moved as if it were embedded in parallel flow. The same may have been true of air near number 4, although it apparently moved nearer the developing eddy. Its motion is less well explained because of the uncertain causes of its plume shape.

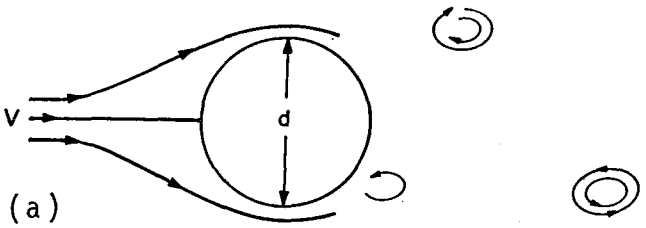

Figure 7. (a) Schematic diagram of a vortex trail produced by an incompressible fluid moving past a solid right circular cylinder under laboratory conditions.

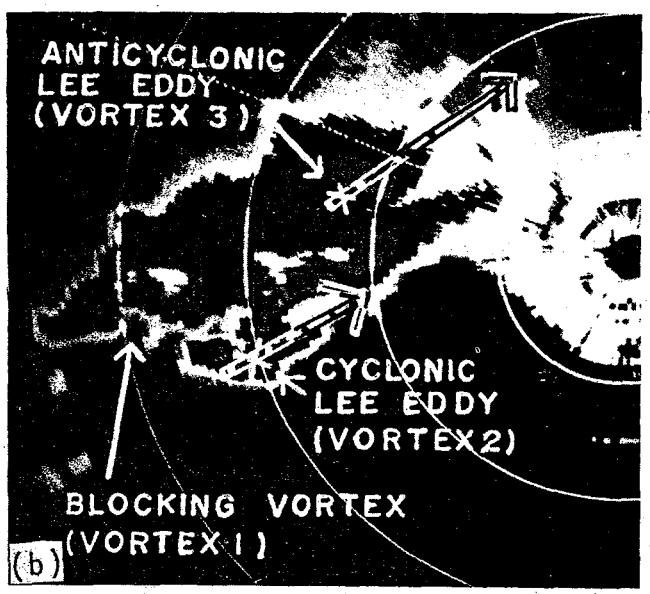

Figure 7. (b) Radar echo patterns at 1620 CST, 25 June 1969 at an antenna elevation of 4°. A Kármán vortex train is resembled if vortices 2 and 3 are considered as lee eddies downstream from vortex 1. Arrows represent the direction of relative motion of the lee eddies from 1616 to 1655. Dots along the arrows indicate approximate 10-min positions of vortex centers. X's represent the centers at photograph time.

4.2 Lee Eddy Generation

Much of the following discussion concerns various aspects of the anticyclonic eddy, and Lemon's paper is the primary source of that information.[2] In the vicinity of the thunderstorm, an attempt was made to construct the horizontal flow pattern at midlevels (near 12,000 ft MSL) both from chaff and from contoured PPI radar presentations. Time-lapse movies indicated three regions of rotation. They are labeled as vortices 1, 2, and 3 in figure 7b. Although horizontal air flow, implied from radar presentations, is difficult to derive and can be misleading, time-lapse movies of this storm indicated that the horizontal precipitation echo motions were consistent with chaff motions. This, together with Lemon's study, indicates that flow patterns implied from PPI presentations represent the horizontal air flow fairly well. Figure 7b condenses the results of the time-lapse film study of this storm. The persistent vortex patterns show a close resemblance to those of lee vortex generation found in laboratory experiments involving fluid flow past a right cylinder. In such a comparison, vortices 1, 2 (cyclonic), and 3 (anticyclonic) replace the cylinder and its lee vortices, respectively.

Experiments (Prandt and Tietjens, 1957) have shown that eddies are generated regularly from a cyclonically rotating cylinder, when the ratio of the cylinder rim speed u to the ambient fluid speed v varies from 0 (stationary) to at least 1/2, and when the Reynolds number of the fluid, $R_e = Vd\rho/\mu$, varies from 10^3 to 10^5, where d is the diameter of the cylinder, ρ is the density of the fluid, and μ is the fluid coefficient of viscosity. Vortices forming on either side of the cylinder, as pictured in figure 7a, have opposite directions of rotation and form a geometric pattern of alternating cyclonic and anticyclonic vortices to the lee of the obstacle. They entrain environment fluid only slowly, move at a speed slower than the ambient flow, and are eventually dissipated by internal friction. Von Karman proved that vortex trails have a geometric pattern that is "generally unstable" resulting in deviations from the pattern seen in figure 7a. Neutral stability occurs at a value of $h/l = 0.28$,

---

[2] Lemon offered three possible explanations for the anticyclonic eddy: (1) it may have been related to a nonsteady rotation of the updraft and was therefore a "starting vortex"; (2) it could have been created by a systematic flow in which the conservation of three-dimensional vorticity was prominent; or (3) it may have been of the Karman-type shed from vortex 2 in figure 7b.

where h and l are the cross distance and wavelength as indicated in the figure. The value of this ratio is difficult to measure accurately when a single vortex pair is present, because the tendency for instability does not allow one to measure h and l with confidence over a long enough time. No estimate for the value of this ratio appears here for the June 25th storm for this reason.

The similarity between the flow pattern of these laboratory experiments and that of figure 7b is striking. At about 1615, storm vortices 2 and 3 became well-defined to the lee and on either side of vortex 1. They rotated in opposite directions and traveled downstream from vortex 1 in a direction very nearly that of the mean wind at midlevels (230°/50 kt) but at a slower speed. Both eddies traveled near 20 kt relative to vortex 1 as the anticyclonic eddy became visible at 1615, but speed differences arose as the anticyclonic eddy accelerated and the cyclonic eddy decelerated. Their relative speeds at 1655 were near 35 and 10 kt, respectively, as precipitation associated with the anticyclonic eddy disappeared.

Although the results of the time-lapse film study are consistent with lee vortex generation, it cannot be resolved whether or not such a phenomenon actually contributed to the circulation of the thunderstorm under study. Evidence both pro and con may be cited. Evidence against vortex generation is the fact that the Reynolds number for the situation on this date was found to be considerably greater (near 10^9) than the critical value determined experimentally (always true for the atmosphere). Laboratory results, however, were based on flow around a solid obstacle by an incompressible fluid. Undoubtedly, a different critical value for the Reynolds number would be found for flow around a vortex composed of the fluid itself, especially in the presence of mixing between the vortex and its surroundings. To the author's knowledge, comparable experiments have not been performed, and no one can reliably say what values of Reynolds number are appropriate.

There is evidence that suggests that Van Karman vortex trails do occur in the atmosphere on this scale. Friday and Wilkins (1967) described vortex trail phenomena in the lee of the Guadalupe and Cape Verde island group. Such trails were observed in the lee of 15 different islands from the Gemini photographs alone. One example appears in figure 8. In this Gemini V photograph, an eddy pattern resembling a Karman vortex trail is present in the lee of Guadalupe Island off the southwestern California coast (maximum height near 4500 ft) at 1414, 21 August 1965. In their study, Friday and Wilkins found two apparent pre-

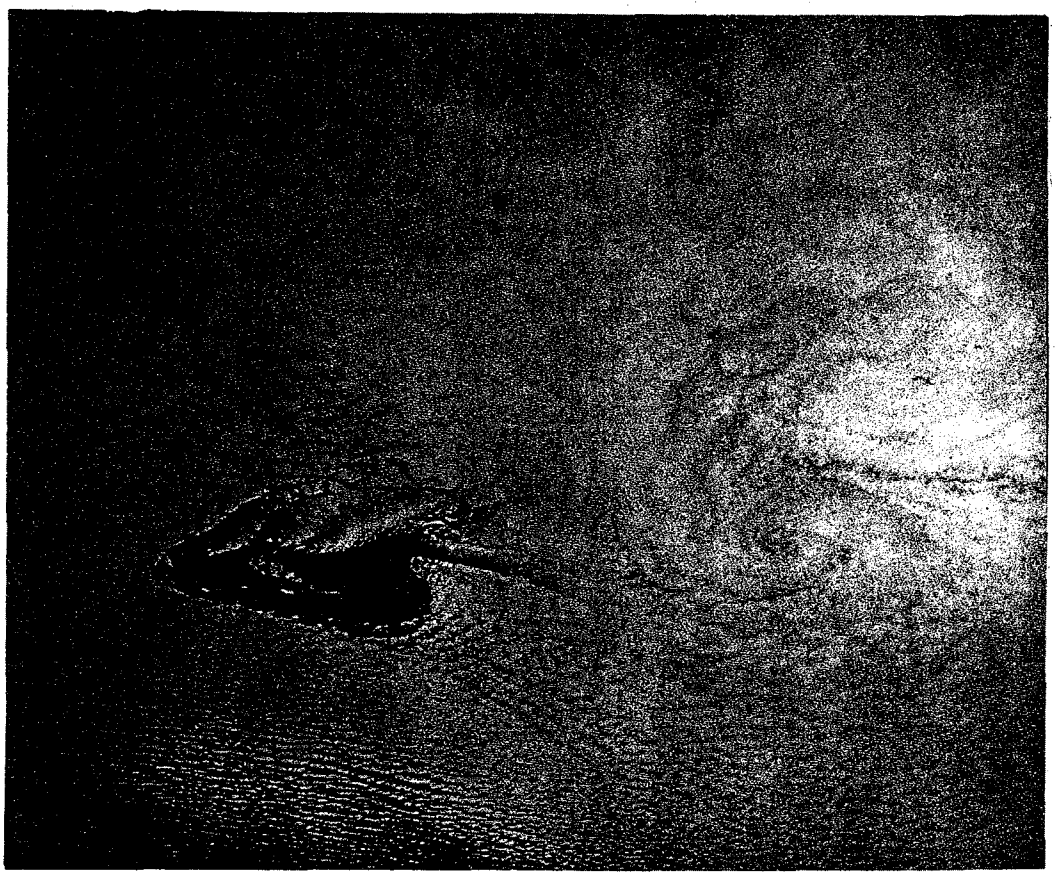

Figure 8. Vortices to lee of Guadalupe Island as photographed from a satellite at 1414, 21 August 1965.

requisites for vortex trail formation: steep slopes or bluff objects and a high degree of vertical stability (an inversion). They believed that the inversion would cause a relatively larger portion of the air to flow around the island instead of over it. These two prerequisites are apparently met near a mature thunderstorm. Vertical updrafts tend to block environmental flow much as steep mountain slopes, and the stratospheric inversion tends to cause environmental air to flow around the updraft rather than over it. Zimmerman's (1969) studies of vortex trails also suggests that much of the Van Karman theory may be successfully applied to atmospheric mesoscale eddy patterns. Other studies have been made by Hubert and Krueger (1962) and Chopra and Hubert (1964,1965).

A study of Fujita and Grandoso (1968) indicates that eddies were observed in the lee of convective thunderstorm towers on 3 April 1964. The contoured radar display of storms on this date led them to propose that wake vortices

developing to the lee of a mature thunderstorm caused it to split into cyclonically and anticyclonically rotating storms that moved to the right and left of the previous trajectory, respectively.

On June 25th, the strongest evidence supporting the vortex generation concept was the behavior of chaff near the storm. The fact that a speed minimum occurred where midlevel air was being deflected just upstream from vortex 1 is significant since this implies that the vortex was capable of blocking environmental flow. Chaff indicated that air was being drawn into an anticyclonic eddy and that downward motion was present near it. Both are consistent with Lemon's analyses A discussion of lee eddy generation within this storm appears later.

The streamline pattern constructed from chaff trajectories at the fringe of the storm generally agrees with with the right-moving mature severe thunderstorm models of Browning-Ludlam (1962), and Fankhauser (1971); this suggests that environmental flow patterns of this storm differed little from these recent models. Storm streamlines are superimposed over schematic representation of these two models in figures 9 and 10. Fankhauser's model is expecially

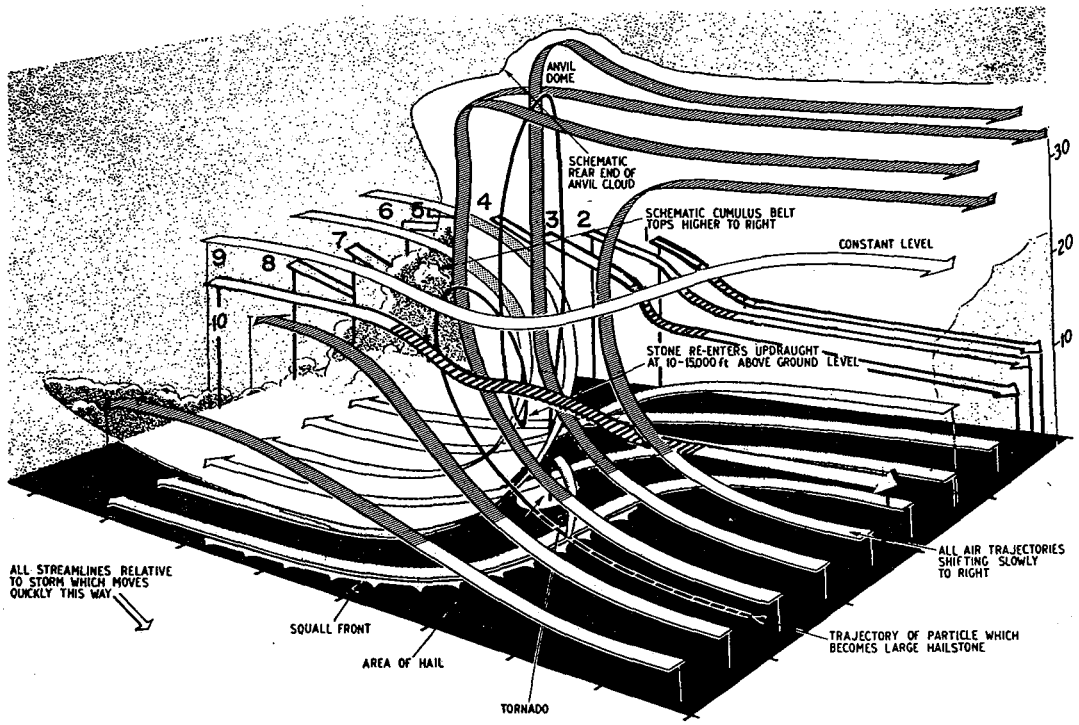

Figure 9. Three-dimensional model of relative airflow within a mature severe thunderstorm (after Browning and Ludlam, 1964). Numbered streamlines were constructed from chaff trajectories; the darkened portions are flow within precipitation.

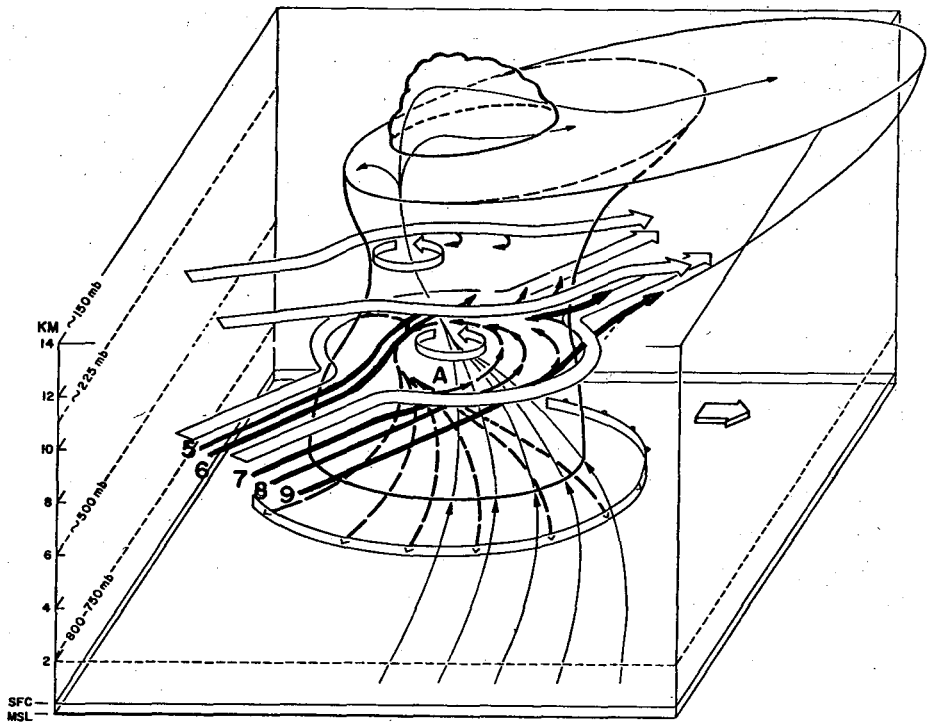

Figure 10. Three-dimensional interpretation (after Faukhauser, 1971) of the interacting external and internal airflow of an individual persistent Great Plains cumulonimbus, accommodating the impressions from earlier works and features observed in two Oklahoma field experiments. The thin, solid inflowing and ascending streamlines represent the history of moist air originating in the subcloud layer (surface to ∿750 mb). The heavy dashed streamlines trace the entry and descent of potentially cold and dry middle-level (700 to 400 mb) air that feeds the downrushing and diverging downdraft. The surface boundary between the inflow and downdraft is shown as a barbed band. The internal circular bands signify net updraft rotation of the downdraft. The shape and orientation of the dividing external bands represent typical vertical shear and character of ambient relative horizontal airflow at middle (∿500 mb) and upper (∿225 mb) levels. The approximate pressure-height relationship is shown at the left. The broad flat arrow on the right represents direction of travel. Solid arrows indicate flow patterns derived from time-lapse movies of chaff echoes.

appropriate since rotation (possibly corresponding to vortex 1) is incorporated. In both models, low-level air along the right rear quadrant of the storm is the main source of updraft air, while midlevel air entering precipitation on the upwind side of the storm is the primary contributor to the downdraft.

Only a small change in these model streamlines is needed to accommodate a flow pattern leading to the development of lee eddies. Let us consider a thunderstorm with a flow similar to that in figure 9. At this stage of maturity no rotation is evident; however, a mechanism that can lead to the development of a vortex is present. Midlevel air entering the upwind side of the storm becomes negatively buoyant as a result of evaporative cooling and rushes downward creating a dome of cool air which tends to spread outward in all directions. The pressure gardient associated with this meso-high extends ahead of the rain-cooled air into the low-level environmental air causing it to be slowed and approach a calm, which is often observed near the edge of the meso-high. This results in cyclonic shear in the environmental air at low levels near the interface where lifting takes place. Lifting releases instability and further convection results. Low-level air converges to replace the lifted air and may enhance the initial cyclonic vorticity. Sufficient convergence may produce a cyclonic vortex (corresponding to vortex 1). We may then have a thunderstorm flow pattern similar to that seen in Fankhauser's model.

It requires only one step more to obtain the Karman vortex train. Figure 11 is a schematic representing an air flow pattern that seems consistent with this next step. It is admittedly speculative and will be difficult for many readers to accept at first reading. It is believed, however, that it is a reasonable explanation and is consistent with the observations and interpretations of the June 25 storm. Consider that midlevel environmental air diverted around the rotating thunderstorm updraft (vortex 1) may have led to the generation of lee eddies at midlevels in much the same way that flow around solid objects generates lee eddies. The column of rotating air associated with the cyclonic lee eddy implies a relative pressure deficit near its vortex center since a continual acceleration (pressure gradient force) is required to deflect air movement from straight line flow. This circumstance induces some degree of upward motion in the column from below and could enhance eddy development at low levels especially if it is above a region of lifting at low levels. This would provide a favored location for cyclonic eddy development from near the surface to midlevels. Storm analyses on June 25th indicated that such a situation was consistent with observation, i.e., a surface meso-high interface extended downstream from the blocking vortex (vortex 1) beneath the region where cyclonic lee eddy generation could be expected. Thus, it seems plausible that vortex 2 may have been generated in this way.

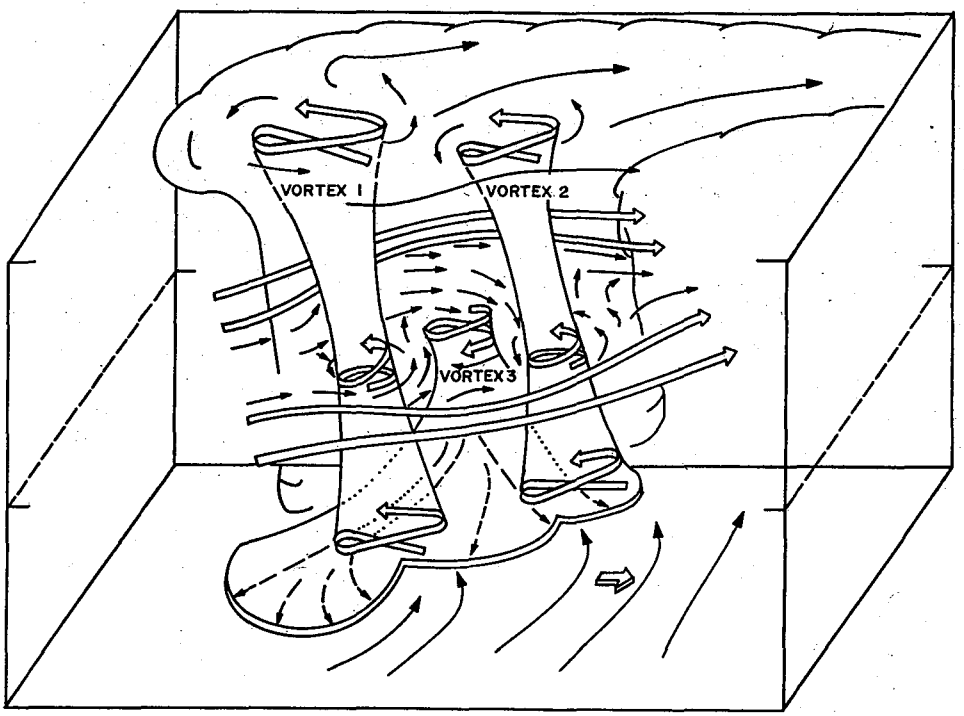

Figure 11. Schematic representing relative flow that is consistent with lee vortex formation. Horizontal flow is represented by solid thin arrows, spiraling vertical motion by double corkscrew arrows, midlevel environmental air by double gently curving arrows, and rain-cooled downrushing air by the dashed arrows that end at the meso-cold front. Storm motion is indicated by the short broad arrow near the bottom of the figure.

Vortex 3, the anticyclonic vortex, may have developed as follows: midlevel air entering precipitation in the lee of the blocking vortex would become rain-cooled and move downward causing the air at midlevels to converge and replace it. In the region of anticyclonic vorticity (generated lee eddy), converging air would enhance this motion so that an anticyclonic downdraft could result (vortex 3). The anticyclonic downdraft described previously in this paper was located near the region where anticyclonic lee eddy generation would be expected. Therefore, it seems reasonable that vortex 3 could have developed in this way.

5. SUMMARY AND CONCLUDING REMARKS

On 25 June 1969, chaff was released upstream from an isolated thunderstorm within which an eddy pattern resembling a Karman vortex train was developing. Relative chaff trajectories provided much of the supporting evidence. A speed minimum was discovered upstream from a hook echo in a region of diffluence indicating resistance to environmental flow. Rough estimates of vertical motion indicated that the anticyclonic lee eddy at midlevels was composed of downward moving air, thus supplementing Lemon's analysis, and some chaff was apparently drawn toward the anticyclonic eddy, indicating convergence. It was particularly interesting to discover that such events seem reasonable with only a slight modification of current severe thunderstorm model flow patterns.

Radar patterns consistent with a development of this kind may not be uncommon. Research of radar film with contoured PPI displays indicates that similar patterns have appeared on a number of occasions during the last several years. When radar-echo contouring becomes established across the U.S., it may be found that such patterns are relatively frequent along thunderstorm lines in which individual storms tend to move along the orientation of the line.

6. 23 JUNE 1969

6.1 Storm History

Two synoptic-scale features were instrumental in producing severe thunderstorms in central Oklahoma on this date A quasi-stationary front positioned across southern Oklahoma at 0600 (fig. 12a) provided a lifting mechanism for low-level moist air flowing northward from the Gulf of Mexico. An upper trough, over New Mexico (fig. 12b) traveled across Oklahoma during the day, enhancing the formation of a weak surface low. Low-level warm advection, indicated by the Tinker AFB 1800 sounding seen in figure 13, also contributed to thunderstorm development. At 1400, as solar heating approached its maximum, thunderstorms began forming near Norman.

Ninety minutes later, an interesting interaction took place among four thunderstorms labeled A,B,C, and D in figure 14. Thunderstorms C and D were traveling toward the nearly stationary thunderstorms A and B, as shown in

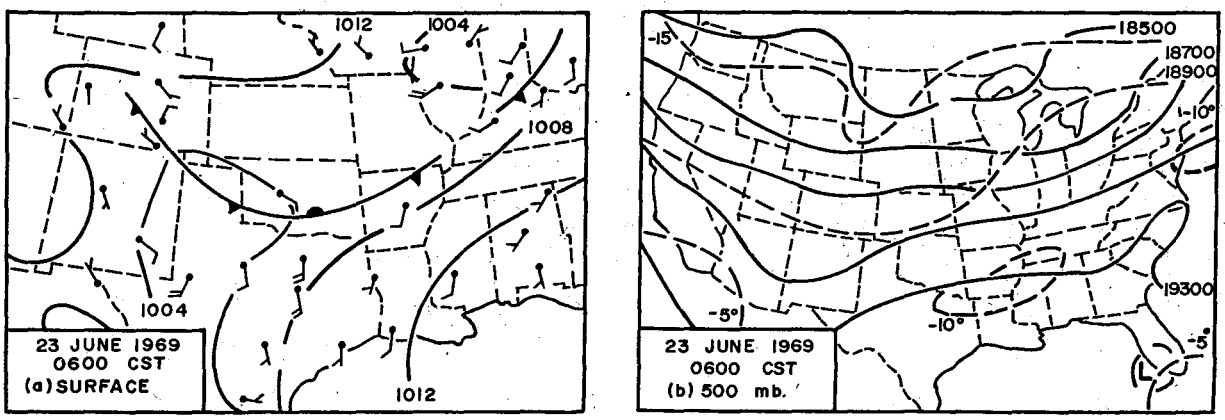

Figure 12. Synoptic charts before thunderstorm formation.

figure 14 radar pictures, and by the storm trajectories appearing in figure 15. The storms were moving about 15° to the left of the environmental flow above 10,000 ft MSL, as a comparison of the trajectories with the 1800 Tinker AFB hodogram indicates. Thunderstorms C and D both had speeds near 25 kt until 1535, when each began to accelerate and decrease in intensity. Thunderstorm D accelerated only

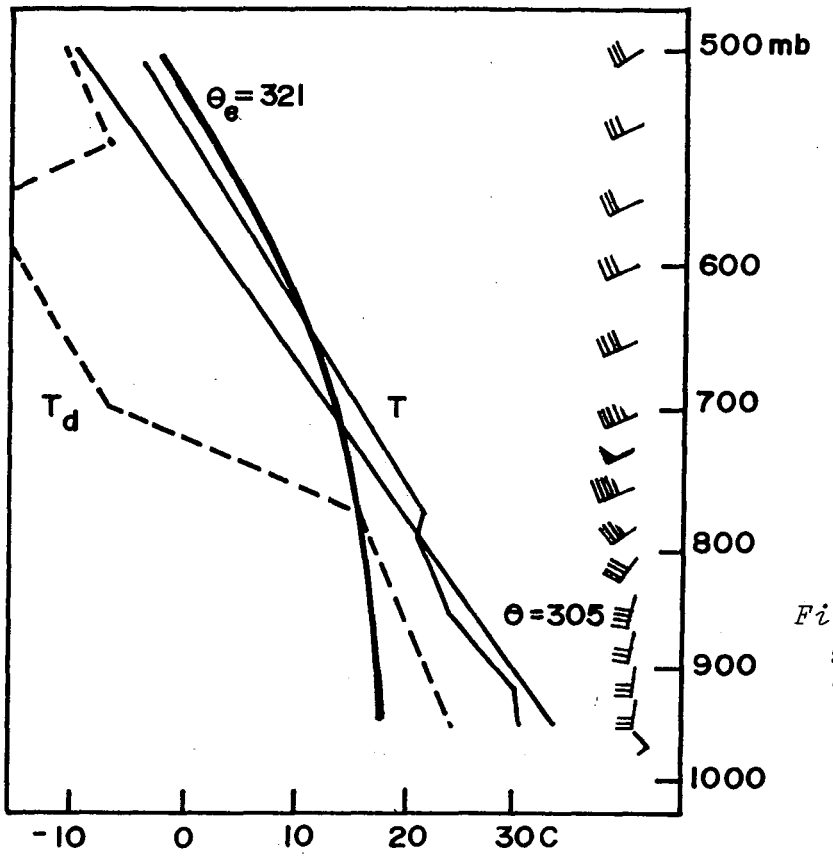

Figure 13. Stüve diagram of Tinker AFB sounding 1800 CST 23 June 1969.

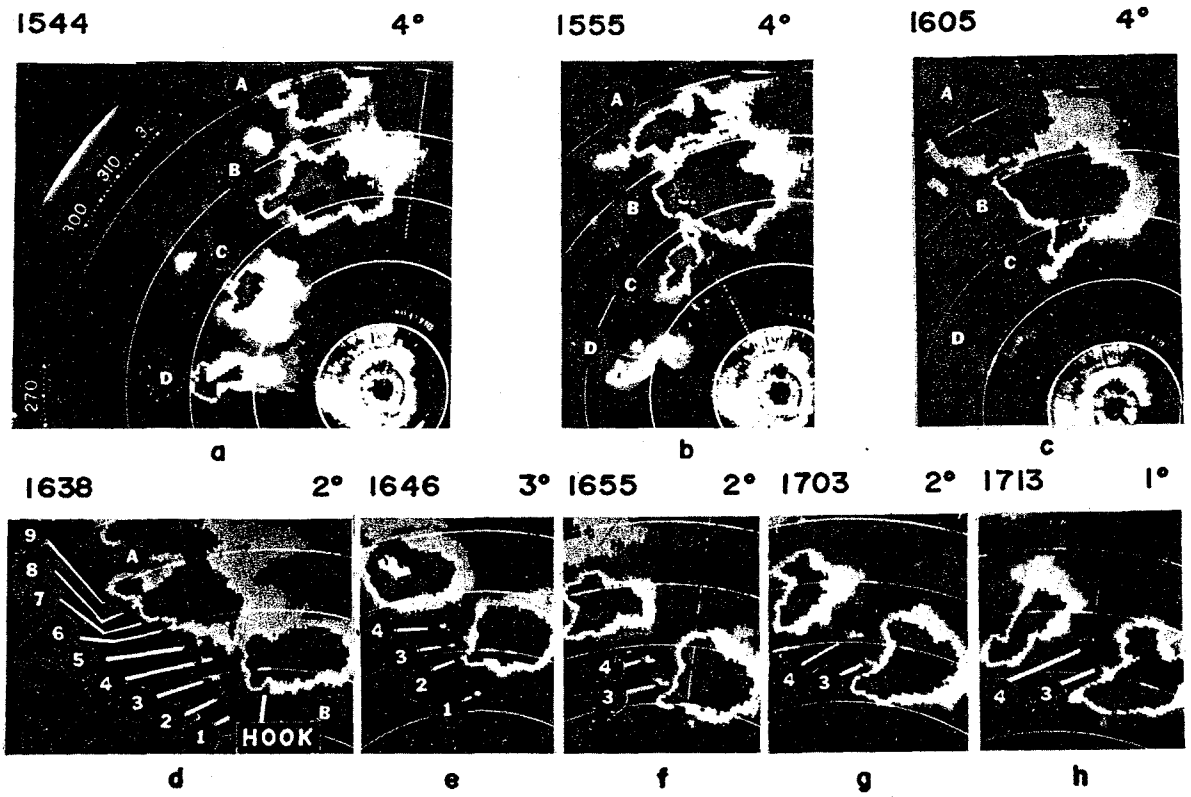

Figure 14. Radar depiction of thunderstorms A, B, C, and D between 1544 and 1713 CST. Thunderstorm C merges with B in the first three photographs. The motion of chaff released near thunderstorms A and B is shown in d through h. Time (CST) marks are at 10 n mile intervals.

slightly and dissipated. Thunderstorm C, however, nearly doubled its speed (to 45 kt) and merged with B at 1605, as shown by the radar PPI displays in figures 14a through 14c. Immediately thereafter, thunderstorms A and B began moving at about 25 kt, separating from each other at an angle of nearly 15°. Almost 2 hr later, at 1750, thunderstorm B produced a tornado that, according to the ESSA Weather Bureau *Storm Data*, did considerable damage at Perkins, Oklahoma, 50 n mi northeast of NSSL.

There is some evidence that thunderstorm C merged with B just to the right of an area of well-organized vertical motion. Radar time-lapse movies indicated cyclonic rotation was centered in thunderstorm B in its right-rear quadrant where low intensity reflectivity ($Z_e < 10^1$) is indicated in figure 16a. The vault, pictured in figure 16b, was at the same location. As noted earlier in section 4, these radar echo features have been associated with regions of well-organized vertical motion.

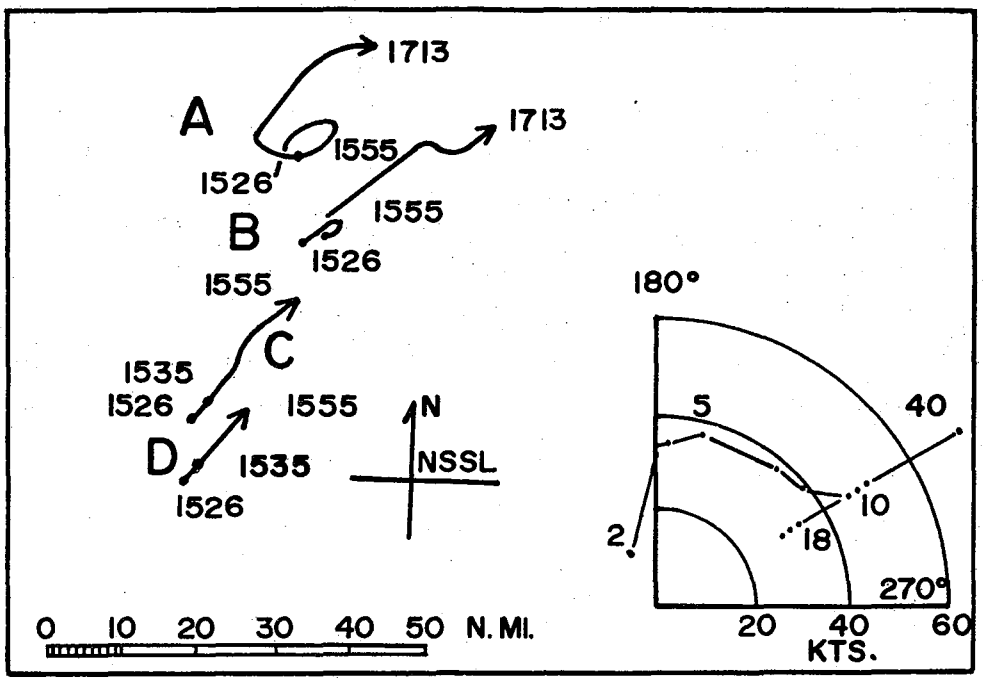

Figure 15. Trajectories of thunderstorms A, B, C, and D. Hodogram on right is 1800 CST Tinker AFB for 23 June 1969.

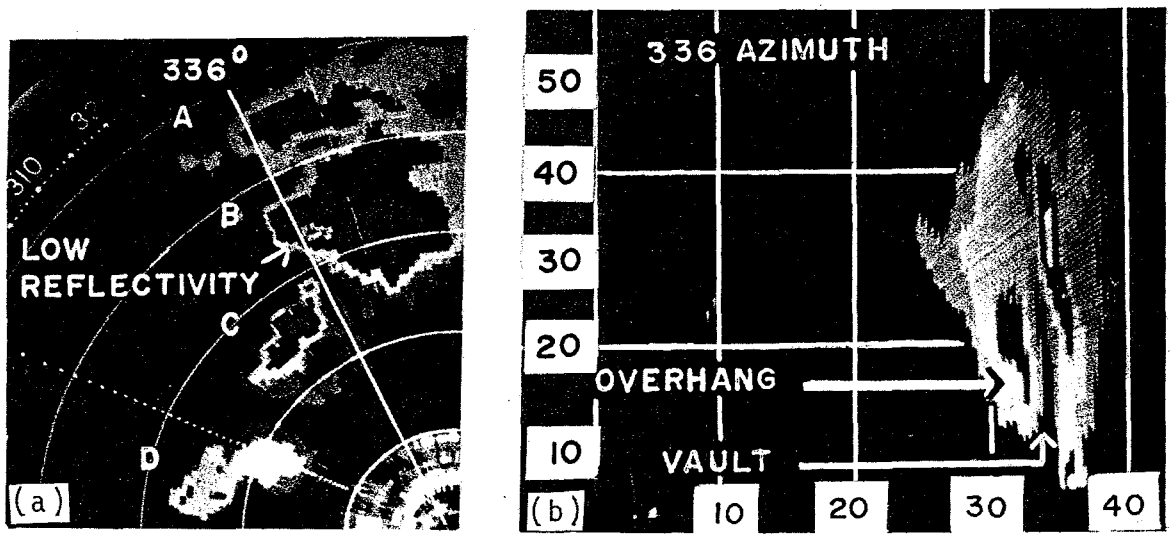

Figure 16(a). PPI photograph at 1553 CST showing a region of low reflectivity encircled by greater intensity reflectivity at 4° tilt. Range marks are at 10 n mile intervals. (b) range-height cross section of thunderstorm B at 1553, 23 June 1969, along azimuth 336° from NSSL.

6.2 Chaff Trajectories and Airflow

Chaff was released near thunderstorms A and B between 1615 and 1630 just as they began separating. Nine bundles were placed at 15,000 ft MSL at 3-n mi intervals, 3 to 5 n mi upstream from these 50,000-ft tall thunderstorms. The chaff echoes appear in figure 14d. Bundles 5, 6, 7, 8, and 9 entered thunderstorm A almost immediately and were never visible again; on the other hand, 1, 2, 3, and 4, remained in view considerably longer and are the subject of the remainder of this section. The relative trajectories of these chaff bundles appear in figure 17. Time-lapse movies of radar echoes revealed local cyclonic rotation in the right-rear quandrants of both thunderstorms at the time of chaff release. A hook-shaped echo in thunderstorm B is visible in figures 14d and 14e. The distance between bundles 1 and 2 increased between 1625 and 1645 as they approached the hook. Later (1645), however, the trajectory of bundle 1 turned to parallel bundle 2 again just before it entered the precipitation echo. This, and the PPI display in figure 4e, suggests a vortex center was located near the edge of the precipitation echo (at X in fig. 17).

It may seem reasonable to expect that regions of strongly reflecting storm cores ($Z_e \geq 10^4$) significantly deflect air near severe thunderstorms since strong up- and downdrafts are located near these cores. Evidence in figure 17 suggests, however, that this was not true in this instance. After deflection of bundles 1 and 2 was no longer apparent, they both traveled toward thunderstorm B at a relative speed of near 30 kt without significant velocity change. This was true although they were merging with the precipitation echo along a trajectory nearly perpendicular to its contours as seen in figures 14e and 14f and implied in figure 17. This suggests that neither the merging angle of the environmental air to contours of precipitation, nor the strong gradient of precipitation intensity was associated with environmental air deflection.

The relative trajectories of bundles 3 and 4 in the regions between thunderstorms A and B are particularly interesting since so little is known about the air flow between two adjacent severe thunderstorms. Chaff entered this region at about 12,000 ft MSL and was visible to about 8,000 ft MSL. Both bundles decelerated and maintained their small relative height differences (fig. 18), so that diffluence

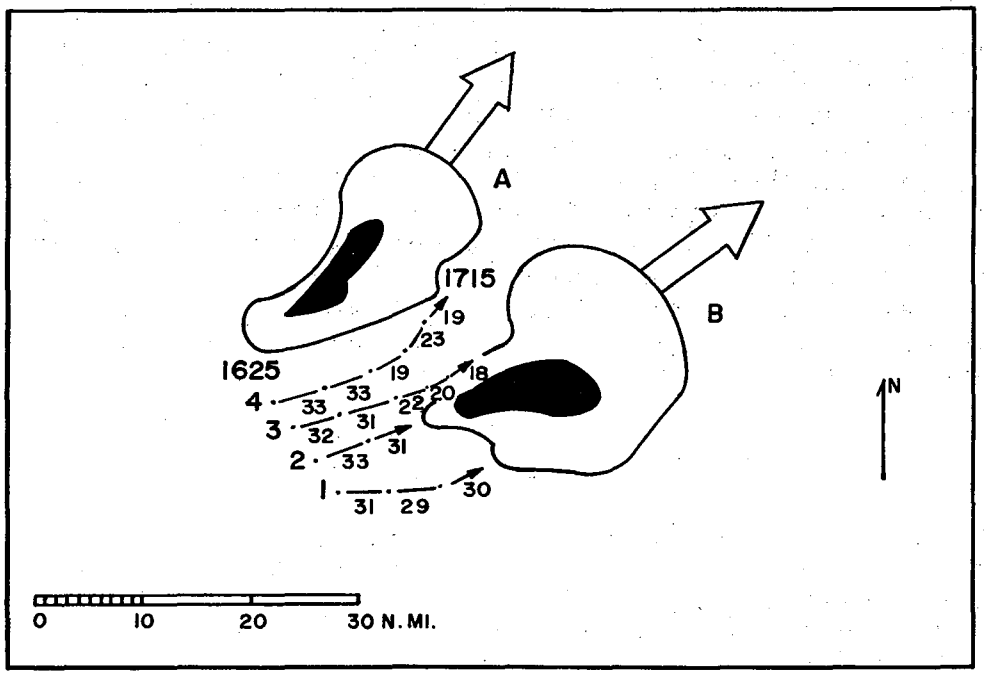

Figure 17. Relative chaff trajectories 23 June 1969. Dots show 10 min chaff positions along the trajectories. Two-digit numbers below trajectory segments are relative speeds (knots). Thunderstorms A and B are shown by composite schematics constructed from radar PPI scope photographs between 1625 and 1755, when the trajectories were observed. The shaded regions depict areas of radar reflectivity $Z_e \geq 10^4$. Double arrows show average storm motion.

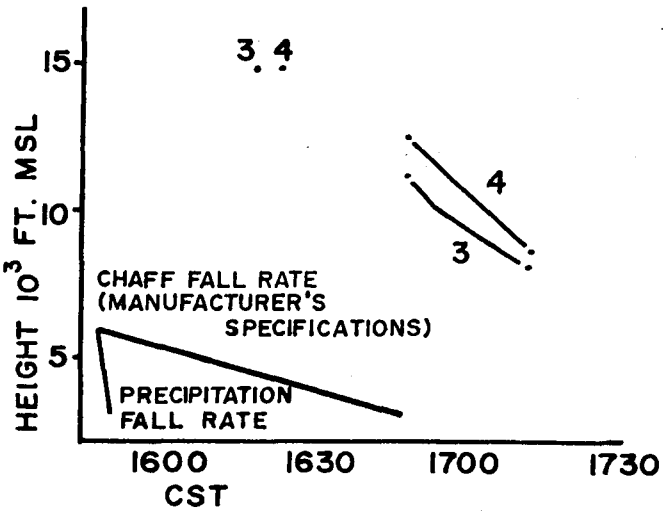

Figure 18. Chaff fall rates. Numbered lines correspond to chaff bundles 3 and 4.

was suggested by their horizontal separation. Chaff fall rates indicated that downward motion in this region was about 2 kt. Strong ventilation of both thunderstorms was evident in figure 17 by the 20 to 30 kt relative speeds of all four chaff bundles as they merged with precipitation. Thus chaff moved as if a region of subsiding diffluent air existed between two partially ventilated thunderstorms. Cooling by evaporation probably contributed to this air flow, since radar indicated that precipitation between these thunderstorms ended just as these bundles approached that region (figs. 14d through 14f).

6.3 Concluding Remarks

Two important similarities were observed between this experiment and the one of 25 June. Thunderstorm B was ventilated at its fringes and air was deflected along its upwind side where vertical motion within the storm was likely well-organized.

The presence of thunderstorm A adjacent to thunderstorm B made it possible to collect air trajectory data in the region between them. Chaff trajectories indicated that flow was diffluent and subsiding, suggesting that these thunderstorms were not acting as solid barriers to flow at the time chaff moved between them. The existence of the subsiding diffluent flow may have been only of short duration, since it was probably due to the effects of precipitation, but it is possible that it was in some way associated with the separation of these storms.

7. 29 MAY 1969

7.1 Synoptic Situation and Brief Storm History

The synoptic patterns on this date were weak and poorly organized, similar to those of early summer that often produce a few moderate to heavy thundershowers. An upper-level trough in Kansas (fig. 19b) contributed to the formation of a weak surface low along the cool front (fig. 19a) as it drifted into Oklahoma. The 1200 Tinker AFB sounding (fig. 20) indicates weak warm air advection below 600 mb, very little cold air advection above, and only weak conditional instability with a gradual decrease of moisture with height.

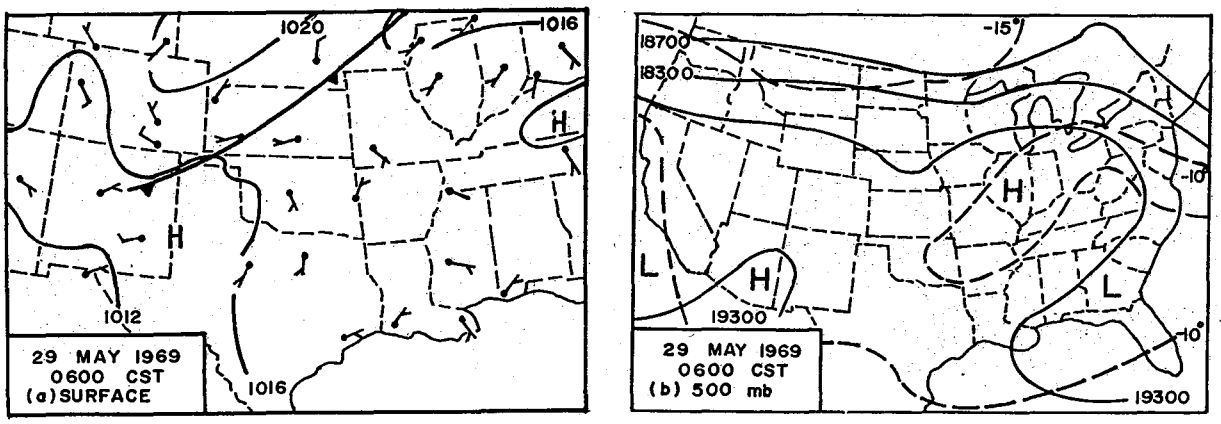

Figure 19. Synoptic charts before thunderstorm formation.

A few thundershowers did form near the front by early afternoon, and by 1400 several thundershowers of moderate intensity were located about 50 n mi north and west of NSSL. They drifted from the northwest at less than 10 kt, reflecting the light flow aloft. By 1600, moderate thundershowers extended along a broken line 100 n mi long and just 30 n mi to the northwest of NSSL (fig. 21a).

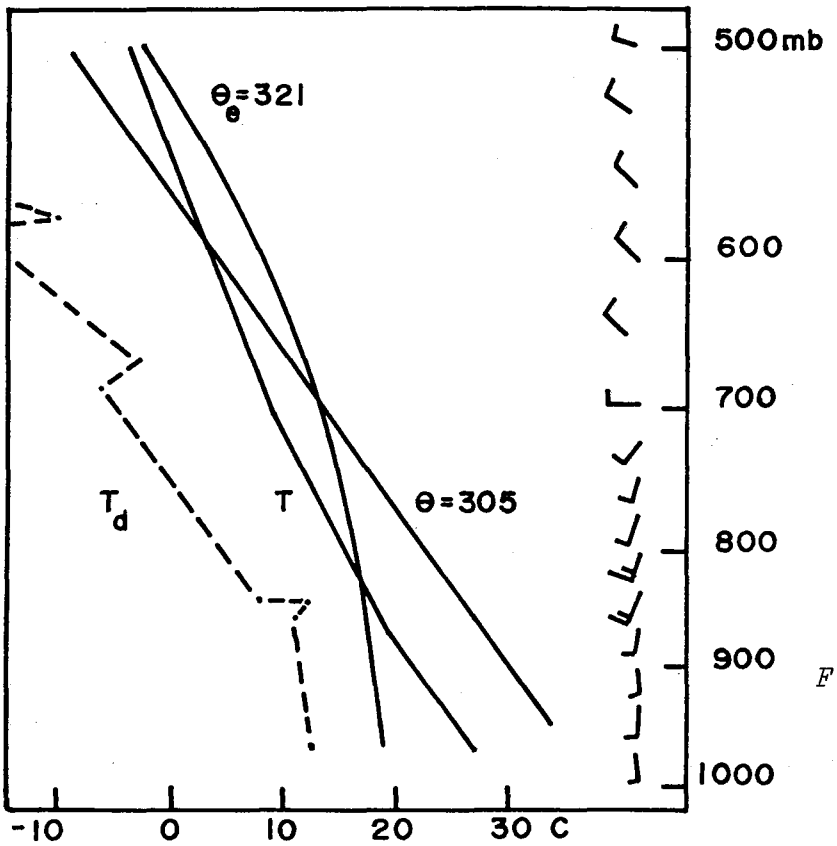

Figure 20. Stüve diagram of Tinker AFB sounding 1200 CST, 29 May 1969.

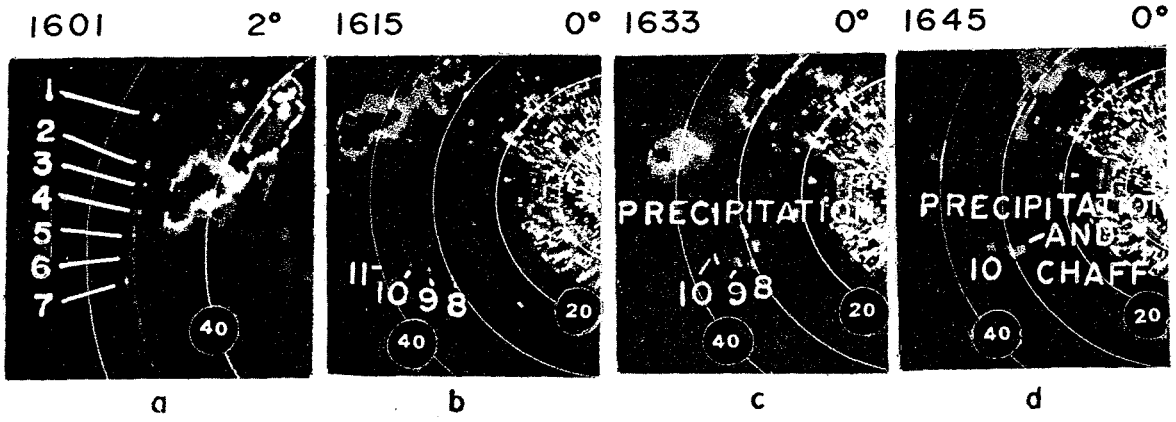

Figure 21. Radar presentation of chaff released on 29 May 1969. (a) Chaff released at 4.5 km MSL to the west of thundershower activity; (b), (c), and (d) Chaff launched at 2 km MSL southeast of the thundershower line. Time of PPI displays and radar antenna tilt are indicated below each figure.

7.2 Chaff Trajectories

Two chaff experiments were initiated for this storm: a repeat of the midlevel ambient flow investigations, and a low-level inflow experiment. Between 1550 and 1615, 11 bundles of chaff were ejected at 3-n mi intervals in the vicinity of thundershowers: seven bundles (fig. 21a) were released from 15,000 ft MSL, 5 to 15 n mi west of the line; four bundles (fig. 21b) were dropped from 5500 ft MSL about 15 n mi southeast of the precipitation. Unfortunately, the thundershowers nearest the chaff dissipated within 45 min after chaff was released.

The motion of chaff at both levels was as anticipated from the wind sounding (fig. 20). The midlevel chaff drifted from the northwest at about 10 kt and low-level chaff moved about 15 kt from the south. Relative chaff trajectories appearing in figure 22 suggest that these thundershowers were not as strongly ventilated at midlevels as were those of the two previously discussed experiments. Little, if any, relative motion toward the thundershower activity was indicated by the midlevel chaff (bundles 1 through 5), since both the chaff and the line of dissipating thundershowers drifted from the northwest with nearly the same speed. Although the speed of bundles 6 and 7 was greater than that of the thundershower line, little relative motion toward the showers was evident since both bundles moved past to the south of the thundershowers.

The chaff released at 5500 ft MSL (bundles 8 through 11) did have relative motion of nearly 10 kt toward the thundershowers, but the significance of this is difficult to assess because the thundershower line was dissipating and bundles 8, 9, and 10 were apparently influenced by other cumulus clouds. The small precipitation echo appearing in figure 21c at 260°/29 n mi drifted from the northwest at about 8 kt and gradually merged with bundles 8 and 9. As these bundles moved in a straight line toward the shower, they also moved slightly toward each other, indicating they were in a region of confluence. These bundles were not distinguishable from the precipitation echo after the merger.

Another precipitation echo that appeared on radar at 1715 (not shown) apparently developed at the location of bundle 10 and masked its movement thereafter. Unfortunately, number 11 disappeared from radar within 5 min after its release and contributed no information to this experiment.

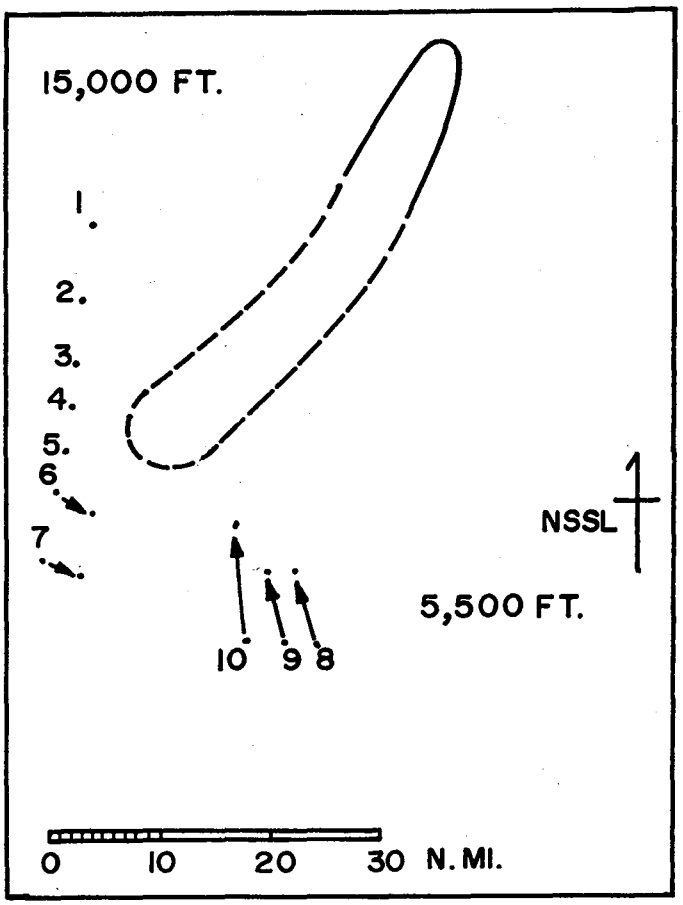

Figure 22. Relative chaff trajectories 29 May 1969. From 1617 to 1717 arrows show the direction of relative chaff motion and a single dot means no motion. The approximate envelope of precipitation echoes is outlined by the dashes, indicating thundershowers that dissipated shortly after chaff was released.

7.3 Concluding Remarks

The most obvious aspect of this experiment was that environment air at midlevels apparently did not interact strongly with the moderately intense ($Z_e = 10^4$) line of dissipating short-lived thundershowers. The low-level chaff drops did not accomplish their intended purpose of providing trajectories for the sub-cloud inflow to the line. They were perhaps dropped too far from the line in view of the convective character of the low-level air in their vicinity.

8. 25 MAY 1969

8.1 Synoptic Conditions and Storm History

The late spring synoptic situation over Oklahoma on May 25th is shown in figure 23a by the dissipating stationary front extending west across the state toward a weak low centered over southwestern Oklahoma, and in figure 23b by a weak 500-mb trough over the Texas-New Mexico border. The Tinker AFB sounding (fig. 24) indicated that the strong westerly flow and large conditional instability frequently associated with Oklahoma severe storms were absent. Air mass thundershowers, however, often form over the state under these circumstances. Those that developed near Norman during the early afternoon on this day remained in the area until near sunset, and one was the subject of a low-level inflow chaff experiment.

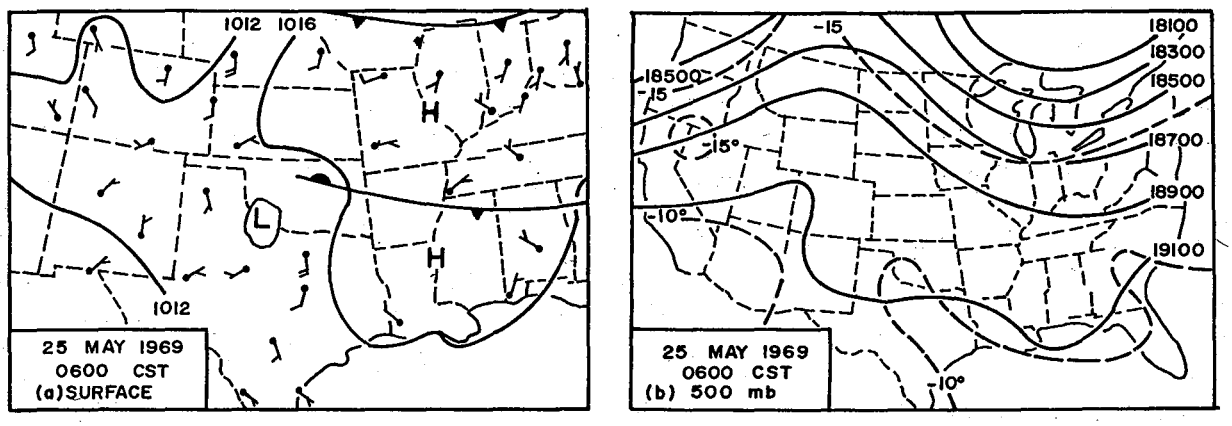

Figure 23. Synoptic charts before thunderstorm formation.

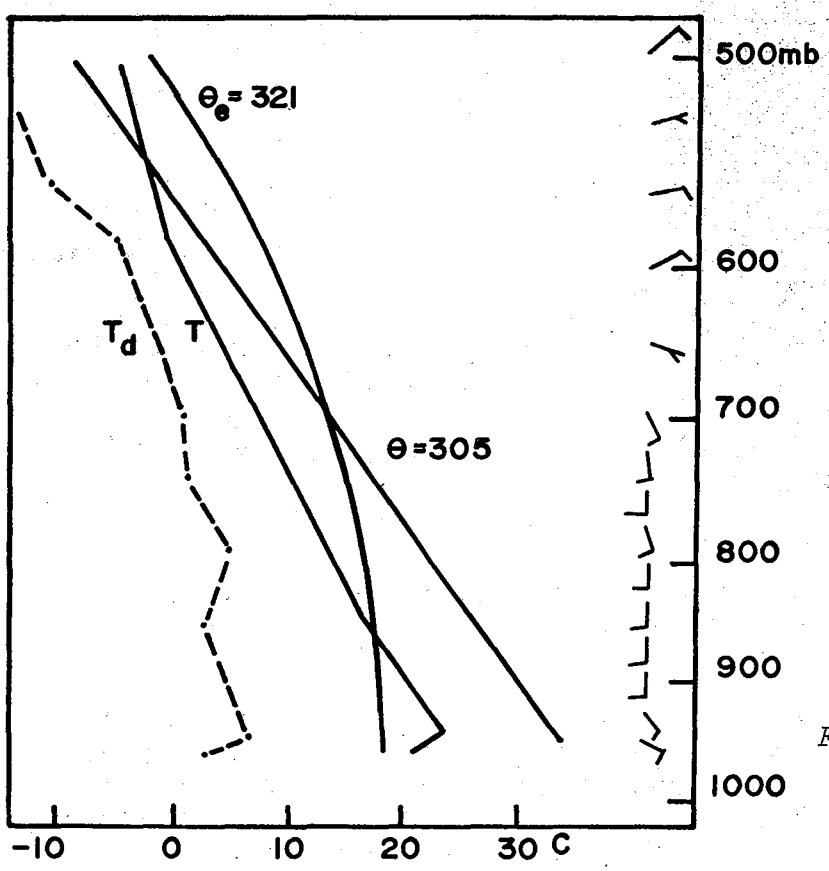

Figure 24. Stüve diagram of Tinker AFB sounding 1800 CST, 25 May 1969.

8.2 Relative Airflow

The thundershower of particular interest developed 20 n mi west of Norman about 1420. It drifted northwest with an initial average velocity of 130°/8 kt, but slowed to nearly half that speed as it reached maturity ($Z_e = 10^5$) 30 n mi west of NSSL. Five chaff bundles (fig. 25) were dropped between 1530 and 1540 at 5000 ft MSL, and at 2-n mi intervals along the upwind (southern) edge of the thundershower as it became mature. Although this shower dissipated within 30 min after the chaff release, some trajectory information was obtained. Relative chaff trajectories shown in figure 26 indicate that low-level air was entering the thundershower all along its upwind side but apparently with some resistance. The trajectories of bundles 3, 4, and 5 suggest that they were released in air being slowed and slightly deflected by the dissipating thundershower. They entered the precipitation at a direction of 30° to the left and at about half the speed (2 kt) of bundles 1 and 2. Bundle 1 remained outside precipitation while bundle 2 merely skirted its edge. These two bundles traveled much

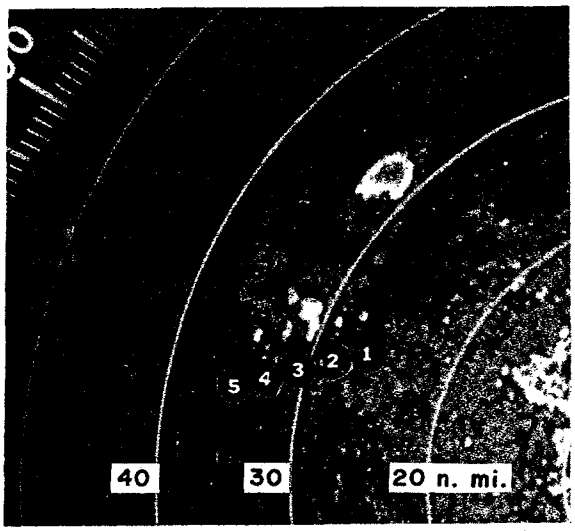

Figure 25. PPI presentation of chaff at 1541 CST, 25 May 1969. Chaff bundles 1 through 5 released between 1530 and 1540 at 1.7 km above MSL.

as the low-level winds would suggest (fig. 24) implying that numbers 3, 4, and 5 were most influenced by the thundershower circulation.

The precipitation echo disappeared from radar shortly after chaff was released, suggesting that the environmental air was deflected around a region of downward flowing air. It is curious that the angle of air deflection was greater near this storm than near the strong, well-organized storm on June 25th. Some contributing factors may have been that the momentum of the environmental air was much less on this date by virtue of the lower wind speed; the areal extent of the blocking flow seemed to be larger and encompassed almost all the precipitation echo; and ventilation appeared to be less. These three factors operating together may have produced this larger angle of deflection.

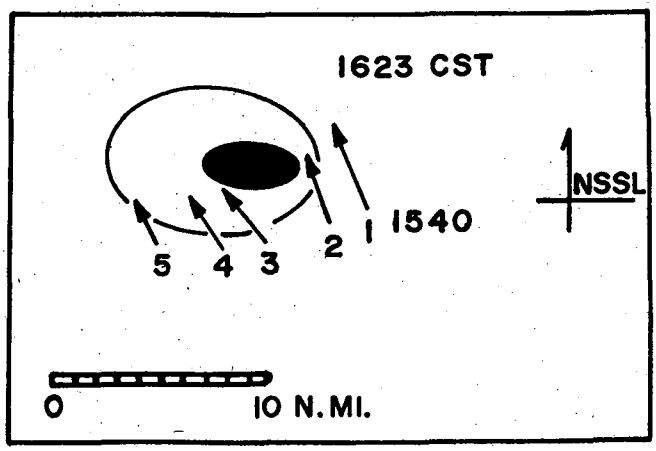

Figure 26. Relative chaff trajectories 25 May 1969. Arrows show relative trajectories of bundles 1 through 5 at 1.7 km near the composite precipitation echo between 1540 and 1623 CST. The dark region is where $Z_e \geq 10^4$ *mm*^{6} *m*$^{-3}$

9. CONCLUDING REMARKS ON THE 1969 CHAFF EXPERIMENTS

Chaff experiments took place on four occasions at NSSL during May and June 1969. Trajectories near severe thunderstorms on June 23 and 25 suggest that strong ventilation at midlevels is characteristic of one type of persistent severe thunderstorm complex. Ventilation at midlevels provides a source of dry air that becomes negatively buoyant as a result of evaporative cooling and moves toward the surface as a cold downdraft, providing a lifting wedge to moist air entering the thunderstorm at low levels. Such events are considered favorable for the maintenance of a thunderstorm over an extended time. The June 25th experiment and surface temperature and potential wet-bulb analyses indicate that midlevel air (although apparently mixed with some low-level air) did reach the ground much as described here.

Blocking of midlevel flow in a relatively small region of the upwind side of severe thunderstorms was noted on occasions when hook echoes were present, implying that vortices and well-organized vertical motion existed there. On one occasion chaff gave supporting evidence to eddies which resembled a Karman vortex train to the lee of a blocking vortex. In the same case a branch of smooth flowing midlevel air entered the storm and became associated with a minor downdraft. Midlevel flow apparently remained smooth while within precipitation, and after it emerged from the storm.

Some insight was gained on the nature of flow at midlevels between two adjacent large severe thunderstorms. Two chaff bundles approaching the thunderstorms, which were separated by 10 to 15 n mi, apparently entered a diffluent region of descending air between the storms. Each bundle entered the precipitation echo of the different thunderstorms. This flow is not characteristic of potential flow between two solid cylindrical barriers.

The importance of these findings is the delineation of the scale on which barrier flow exists in severe thunderstorms. At midlevels only a region of small areal extent near the active organized updrafts exhibits this type of flow. The bulk of the precipitation echo is apparently well ventilated by the ambient flow.

The chaff experiments studied here were intended as a pilot study to test the feasibility of obtaining and analyzing chaff data in the thunderstorm environs. Future experiments should supply additional information in other regions of severe thunderstorms, such as the flow around or through the anvil, and in the sub-cloud inflow layer. Chaff is an inexpensive tracer for determining horizontal trajectories both near and, on some occasions, in thunderstorms. In addition, qualitative information on dispersion rates is obtainable. Finally, the combination of information obtained from chaff trajectories with data from other sources (Doppler radar, surface, aircraft, and sounding data) should provide a more complete picture of severe thunderstorm morphology.

10. ACKNOWLEDGEMENTS

The author expresses thanks to Drs. Edwin Kessler, Stanley L. Barnes, and C. L. Jordan for their constructive criticism and encouragement; to Mr. Ronald L. Shelton, whose patience and desire for perfection made it possible for good quality time-lapse movies to be produced; to Mr. Joseph Golden, who provided the satellite photograph; and to Mr. Charles G. Clark, who prepared the figures.

A special debt of gratitude is owed to Mr. Neil B. Ward who is always ready to share his knowledge and understanding of the atmosphere.

11. REFERENCES

Browning, K.A. (1964), Airflow and precipitation trajectories within severe local storms which travel to the right of the winds, J. Atmos. Sci. 21, 634-639.

Browning, K.A., and F.M. Ludlam (1962), Airflow in convective storms, Quart. J. Roy. Meteorol. Soc. 88, 117-135.

Browning, K.A., and R.J. Donaldson, Jr. (1963), Airflow and structure of a tornadic storm, J. Atmos. Sci. 20, 533-545.

Chopra K., and L.F. Hubert (1964), Karman vortex-streets in the earth's atmosphere, Nature 203, 1341-1343.

Chopra, K., and L.F. Hubert (1965), Mesoscale eddies in wake of islands, J. Atmos. Sci. 22, 652-657.

Donaldson, R.J., R.M. Armstrong, A.C. Chmela, and M. J. Kraus (1969), Doppler radar investigation of air flow and shear within severe thunderstorm, Preprint of Sixth Conf. on Severe Local Storms, pp. 146-154, Am. Meteorol. Soc., Boston, Mass.

Fankhauser, J.C. (1964), On the motion and predictability of convective storms, NSSL Proj. Rept. No. 21, U.S. Weather Bureau.

Fankhauser, J. C. (1968), Thunderstorm-environment interactions revealed by chaff trajectories in the midtroposphere, NSSL Tech. Memo. No. 39.

Fankhauser, J.C. (1971), Thunderstorm-environment interactions determined from aircraft and radar observations, Mon. Wea. Rev. 99, 171-192.

Friday, E.W., and E.M. Wilkins (1967), Experimental investigation of atmospheric wake vortex trails, Res. Inst. Rept. ARL-1576-3, Univ. of Oklahoma, Norman, Okla.

Fujita, T. (1958), Mesoanalysis of the Illinois tornadoes of 9 April 1953, J. Meteorol. 15, 288-296.

Fujita, T., and H. Grandoso (1968), Split of a thunderstorm into anticyclonic and cyclonic storms and their motion as determined from numerical model experiments, J. Atmos. Sci. 25, 416-439.

Gunn, R., and G.D. Kinzer (1948), The terminal velocity of fall for water droplets in stagnant air, J. Meteorol. 6, 243-248.

Hammond, G.H. (1967), Study of a left-moving thunderstorm on 23 April 1964, NSSL Tech. Memo 31.

Harrold, T.W. (1966), A note on the development and movement of storm over Oklahoma on May 27, 1965, NSSL Tech. Memo 29.

Hitschfeld, W. (1960), The motion and erosion of convective storms in severe vertical wind shear, J. Meteorol. 17, 270-282.

Hubert, L.F., and A.F. Krueger (1962), Satellite pictures of mesoscale eddies, Monthly Weather Rev. 90, 457.

Humphreys, W.J. (1940), Physics of the Air (McGraw-Hill Book Co., Inc., New York, N.Y.).

Kraus, M.J. (1970), Doppler radar investigation of flow patterns within severe thunderstorms, Preprints of 14th Radar Meteorol. Conf., pp. 127-132, Am. Meteorol. Soc., Boston, Mass.

Lemon, L.R. (1970), Formation and emergence of an anticyclonic eddy with a severe thunderstorm as revealed by radar and surface data, Preprints of 14th Radar Meteorol. Conf. pp. 323-328, Am. Meteorol. Soc., Boston, Mass.

Mueller, E.A., and A.L. Sims (1966), Investigation of the quantitative determination of point and areal precipitation by radar echo measurements, Atmos. Sci. Lab. Tech. Rept. ECOM-00032-F, Illinois State Water Survey, Urbana, Ill.

Newton, C.W., and S. Katz (1958), Movement of large convective rainstorms in relation to winds aloft, Bull. Am. Meteorol. Soc. 39, 129-136.

Prandtl, L., and O.G. Tietjens (1957), Applied Hydro- and Aeromechanics (Dover Publications, Inc., New York, N.Y.).

Sirmans, D., W.L. Watts, and J. Horwedel (1970), Weather radar signal processing and recording at the National Severe Storms Laboratory, IEEE Trans. Geosci. Electron. GE-8, 88-94.

Stout, G.E., and H.W. Hiser (1955), Radarscope interpretations of wind, hail, and heavy rainstorms between May 27 and June 8, 1964, Bull. Am. Meteorol. Soc. 36, 519-527.

U.S. Weather Bureau (1969), Storm Data 11, No. 6, 76 and 77, U.S. Government Printing Office, Washington, D.C.

Wilk, K.E., W. L. Watts, D. Sirmans, R.M. Lhermitte, E. Kessler, and K. C. Gray (1968), Radar measurements of precipitation for hydrological purposes, World Meteorol. Organization (IHD), Rept. No. 5, 30-46.

Zimmerman, L.I. (1969), Atmospheric wake phenomena near the Canary Islands, J. App. Meteorol. 8, 896.

NATIONAL SEVERE STORMS LABORATORY

The NSSL Technical Memoranda, beginning with No. 28, continue the sequence established by the U. S. Weather Bureau National Severe Storms Project, Kansas City, Missouri. Numbers 1-22 were designated NSSP Reports. Numbers 23-27 were NSSL Reports, and 24-27 appeared as subseries of Weather Bureau Technical Notes. These reports are available from the National Technical Information Service, Operations Division, Springfield, Virginia 22151, for $3.00, and a microfiche version for $0.95. NTIS numbers are given below in parentheses.

No. 1 National Severe Storms Project Objectives and Basic Design. Staff, NSSP. March 1961. (PB-168207)

No. 2 The Development of Aircraft Investigations of Squall Lines from 1956-1960. B. B. Goddard. (PB-168208)

No. 3 Instability Lines and Their Environments as Shown by Aircraft Soundings and Quasi-Horizontal Traverses. D. T. Williams. February 1962. (PB-168209)

No. 4 On the Mechanics of the Tornado. J. R. Fulks. February 1962. (PB-168210)

No. 5 A Summary of Field Operations and Data Collection by the National Severe Storms Project in Spring 1961. J. T. Lee. March 1962. (PB-165095)

No. 6 Index to the NSSP Surface Network. T. Fujita. April 1962. (PB-168212)

No. 7 The Vertical Structure of Three Dry Lines as Revealed by Aircraft Traverses. E. L. McGuire. April 1962. (PB-168213)

No. 8 Radar Observations of a Tornado Thunderstorm in Vertical Section. Ralph J. Donaldson, Jr. April 1962. (PB-174859)

No. 9 Dynamics of Severe Convective Storms. Chester W. Newton. July 1962. (PB-163319)

No. 10 Some Measured Characteristics of Severe Storms Turbulence. Roy Steiner and Richard H. Rhyne. July 1962. (N62-16401)

No. 11 A Study of the Kinematic Properties of Certain Small-Scale Systems. D. T. Williams. October 1962. (PB-168216)

No. 12 Analysis of the Severe Weather Factor in Automatic Control of Air Route Traffic. W. Boynton Beckwith. December 1962. (PB-168217)

No. 13 500-Kc./Sec. Sferics Studies in Severe Storms. Douglas A. Kohl and John E. Miller. April 1963. (PB-168218)

No. 14 Field Operations of the National Severe Storms Project in Spring 1962. L. D. Sanders. May 1963. (PB-168219)

No. 15 Penetrations of Thunderstorms by an Aircraft Flying at Supersonic Speeds. G. P. Roys. Radar Photographs and Gust Loads in Three Storms of 1961 Rough Rider. Paul W. J. Schumacher. May 1963. (PB-168220)

No. 16 Analysis of Selected Aircraft Data from NSSP Operations, 1962. T. Fujita. May 1963. (PB-168221)

No. 17 Analysis of Methods for Small-Scale Surface Network Data. D. T. Williams. August 1963. (PB-168222)

No. 18 The Thunderstorm Wake of May 4, 1961. D. T. Williams. August 1963. (PB-168223)

No. 19 Measurements by Aircraft of Condensed Water in Great Plains Thunderstorms. George P. Roys and Edwin Kessler. July 1966. (PB-173048)

No. 20 Field Operations of the National Severe Storms Project in Spring 1963. J. T. Lee, L. D. Sanders and D. T. Williams. January 1964. (PB-168224)

No. 21 On the Motion and Predictability of Convective Systems as Related to the Upper Winds in a Case of Small Turning of Wind with Height. James C. Fankhauser. January 1964. (PB168225)

No. 22 Movement and Development Patterns of Convective Storms and Forecasting the Probability of Storm Passage at a Given Location. Chester W. Newton and James C. Fankhauser. January 1964. (PB-168226)

No. 23 Purposes and Programs of the National Severe Storms Laboratory, Norman, Oklahoma. Edwin Kessler. December 1964. (PB-166675)

No. 24 Papers on Weather Radar, Atmospheric Turbulence, Sferics, and Data Processing. August 1965. (AD-621586)

No. 25 A Comparison of Kinematically Computed Precipitation with Observed Convective Rainfall. James C. Fankhauser. September 1965. (PB-168445).

No. 26 Probing Air Motion by Doppler Analysis of Radar Clear Air Returns. Roger M. Lhermitte. May 1966. (PB-170636)

No. 27 Statistical Properties of Radar Echo Patterns and the Radar Echo Process. Larry Armijo. May 1966. The Role of the Kutta-Joukowski Force in Cloud Systems with Circulation. J. L. Goldman. May 1966. (PB-170756)

No. 28 Movement and Predictablity of Radar Echoes. James Warren Wilson. November 1966. (PB-173972)

No. 29 Notes on Thunderstorm Motions, Heights, and Circulations. T. W. Harrold, W. T. Roach, and Kenneth E. Wilk. November 1966. (AD-644899)

No. 30 Turbulence in Clear Air Near Thunderstorms. Anne Burns, Terence W. Harrold, Jack Burnham, and Clifford S. Spavins. December 1966. (PB-173992)

No. 31 Study of a Left-Moving Thunderstorm of 23 April 1964. George R. Hammond. April 1967. (PB-174681)

No. 32 Thunderstorm Circulations and Turbulence from Aircraft and Radar Data. James C. Fankhauser and J. T. Lee. April 1967. (PB-174860)

No. 33 On the Continuity of Water Substance. Edwin Kessler. April 1967. (PB-175840)

No. 34 Note on the Probing Balloon Motion by Doppler Radar. Roger M. Lhermitte. July 1967. (PB-175930)

No. 35 A Theory for the Determination of Wind and Precipitation Velocities with Doppler Radars. Larry Armijo. August 1967. (PB-176376)

No. 36 A Preliminary Evaluation of the F-100 Rough Rider Turbulence Measurement System. U. O. Lappe. October 1967. (PB-177037)

No. 37 Preliminary Quantitative Analysis of Airborne Weather Radar. Lester P. Merritt. December 1967. (PB-177188)

No. 38 On the Source of Thunderstorm Rotation. Stanley L. Barnes. March 1968. (PB-178990)

No. 39 Thunderstorm - Environment Interactions Revealed by Chaff Trajectories in the Mid-Troposphere. James C. Fankhauser. June 1968. (PB-179659)

No. 40 Objective Detection and Correction of Errors in Radiosonde Data. Rex L. Inman. June 1968. (PB-180284)

No. 41 Structure and Movement of the Severe Thunderstorms of 3 April 1964 as Revealed from Radar and Surface Mesonetwork Data Analysis. Jess Charba and Yoshikazu Sasaki. October 1968. (PB-183310)

No. 42 A Rainfall Rate Sensor. Brian E. Morgan. November 1968. (PB-183979)

No. 43 Detection and Presentation of Severe Thunderstorms by Airborne and Ground-Based Radars: A Comparative Study. Kenneth E. Wilk, John K. Carter, and J. T. Dooley. February 1969. (PB-183572)

No. 44 A Study of a Severe Local Storm of 16 April 1967. George Thomas Haglund. May 1969. (PB-184-970)

No.45 On the Relationship Between Horizontal Moisture Convergence and Convective Cloud Formation. Horace R. Hudson. March 1970. (PB-191720)

No. 46 Severe Thunderstorm Radar Echo Motion and Related Weather Events Hazardous to Aviation Operations. Peter A. Barclay and Kenneth E. Wilk. June 1970. (PB-192498)

No. 47 Evaluation of Roughness Lengths at the NSSL-WKY Meteorological Tower. Leslie D. Sanders and Allen H. Weber. August 1970. (PB-194587)

No. 48 Behavior of Winds in the Lowest 1500 ft in Central Oklahoma: June 1966 - May 1967. Kenneth C. Crawford and Horace R. Hudson. August 1970.

No. 49 Tornado Incidence Maps. Arnold Court. August 1970. (COM-71-00019)

No. 50 The Meteorologically Instrumented WKY-TV Tower Facility. John K. Carter. September 1970. (COM-71-00108)

No. 51 Papers on Operational Objective Analysis Schemes at the National Severe Storms Forecast Center. Rex L. Inman. November 1970. (COM-71-00136)

No.52 The Exploration of Certain Features of Tornado Dynamics Using a Laboratory Model. Neil B. Ward. November 1970. (COM-71-00139)

No.53 Rawinsonde Observation and Processing Techniques at the National Severe Storms Laboratory. Stanley L. Barnes, James H. Henderson and Robert J. Ketchum. April 1971.

No. 54 Model of Precipitation and Vertical Air Currents. Edwin Kessler and William C. Bumgarner. June 1971.

No. 55 The NSSL Surface Network and Observations of Hazardous Wind Gusts. Operations Staff. June 1971.

GPO 839-618